Carbohydrate Polymers

Newly crosslinked chitosan- and chitosan-pectin-based hydrogels with high antioxidant and potential anticancer activity

--Manuscript Draft--

Manuscript Number:	CARBPOL-D-21-04557R3
Article Type:	Research Paper
Keywords:	monoaldehyde; Polyelectrolyte complex; bioactive glass; polyphenols; micro-computed tomography
Corresponding Author:	Michal Dziadek Akademia Górniczo-Hutnicza im Stanislawa Staszica w Krakowie: Akademia Gorniczo-Hutnicza imienia Stanislawa Staszica w Krakowie Krakow, POLAND
First Author:	Michal Dziadek
Order of Authors:	Michal Dziadek
	Kinga Dziadek
	Szymon Salagierski
	Mariola Drozdowska
	Andrada Serafim
	Izabela-Cristina Stancu
	Piotr Szatkowski
	Aneta Kopec
	Izabella Rajzer
	Timothy E. L. Douglas
	Katarzyna Cholewa-Kowalska
Abstract:	Monoaldehydes, due to natural origin and therapeutic activity, have attracted great attention for their ability to crosslink chitosan hydrogels for biomedical applications. However, most studies have focused on single-component hydrogels. In this work, chitosan-based hydrogels, crosslinked for the first time with 2,3,4-trihydroxybenzaldehyde (THBA), were modified with pectin (PC), bioactive glass (BG), and rosmarinic acid (RA). All of these were not only involved in the crosslinking, but also modulated properties or imparted completely new ones. THBA functioned as a crosslinker, resulting in improved mechanical properties, high swelling capacity and delayed degradation and also imparted high antioxidant activity and antiproliferative effect on cancer cells without cytotoxicity for normal cells. Hydrogels containing PC showed enhanced mechanical strength, while the combination with BG gave improved stability in PBS. All hydrogels modified with BG exhibited the ability to mineralize in SBF. The addition of RA enhanced antioxidant and anticancer activities and promoting the mineralisation process.

30th March 2022

Dear Prof. McCarthy,

Thank you very much for giving us the chance to submit a revision of our manuscript entitled ***Newly crosslinked chitosan- and chitosan-pectin-based hydrogel biomaterials with high antioxidant and potential anticancer activity***. The manuscript has been improved according to the Reviewers' suggestions. Changes which have been made in the manuscript are marked in red. We really hope that this manuscript will be acceptable for publication in ***Carbohydrate Polymers***.

Many thanks for your attention and we look forward to hearing from you.

Yours sincerely

Michal Dziadek (corresponding author) and co-authors

30th March 2022

We were grateful to receive all the valuable comments from the Reviewers. The manuscript has been improved according to the Reviewers' suggestions. Changes which have been made in the manuscript are marked in red. We really hope that this manuscript will be acceptable for publication in *Carbohydrate Polymers*.
Below you will find our detailed answers to the Reviewers' comments and suggestions.

Yours sincerely
Michal Dziadek (corresponding author) and co-authors

Reviewer #2

Overall, the improvements of CARBPOL-D-21-04557R2 over the original submission are massive. I recommend this manuscript for publication since, as the authors state, crosslinkers in which one end is capable of covalent bonding while the other end establishes other kinds of interactions are usually overlooked. To my judgment, the authors have addressed the suggestions with commitment and acceptably defended their position when necessary. I also should acknowledge the comments from the other reviewers in what pertains to enhancing and clarifying the original version.

Thank you for all your comments that allowed us to improve the manuscript.

Reviewer #3

After revision, all the questions raised have been answered. Especially, the molecular interactions and hydrogel structure were elucidated clearly. The manuscript could be accepted after minor revision. Some question presented as follows:

1-How to mill for obtaining the BG with 1 μM because of the importance of its size ? What equipment was used? Please add the detailed method and manufacturers.

2-The particle size distribution was measured by DLS as shown Figure A.1. The DLS method and instrument should be given.

The details have been added in the Materials and methods section.

3-The significant letters/numerals in Fig. 4 should be clearly illustrated. This requires some editing for more clarity.

Figure 4 has been edited for better clarity of the significant letters/numerals.

4-Line 248-251: "The use of monoaldehydes as crosslinking agent of chitosan is not common." But subsequently the author said "several monoaldehydes have been used as crosslinking agents for chitosan-based hydrogels". Obviously, this is paradoxical. This requires some editing for more clarity.

According to the Reviewer's suggestion, the sentences have been revised.

5-The sections in Line 273-285 should be moved to the corresponding discussion sections, not here.

According to the Reviewer's suggestion, the sections in Line 273-285 have been moved.

6-The cited reference style in the text should be revised, such as Line 358 and 363.

The cited reference style has been revised through the manuscript.

Reviewer #5

Abstract section didn't show the key findings and important data, which is a big part of understanding the research.

The abstract was previously revised according to the other reviewers' suggestions. Please note that there are some limitations on the length of the abstract (150 words) that do not allow us to present and summarize all data and results. Furthermore, according to one Reviewer's suggestion, we highlighted the novelty of work in the abstract.

Where is the TGA data?

TG data is included in Appendix – Figure A.4.

It is very difficult to determine the formation of C=N by using FT-IR. Please provide the XPS data to verify the FTIR results.

XPS data for THBA-containing CS hydrogel has been provided and commented to verify the formation of C=N. XPS data is included in Appendix – Figure A.3.

Reviewer #6

The manuscript quality has been improved. Please see the comments in the followings:

Though the abstract has been edited, its writing needs to be improved.

We have rewritten the abstract and made stylistic changes to improve the clarity

The figures are supposed to be placed somewhere close to their discussions. For example, line 259-269 discusses the components and architecture of hydrogel, and it will be helpful to put the hydrogel cartoon (in figure 1) next to it. Similar issues also happen to the other figures.

The figure 1 has been split into two separate ones and the schematic illustration of the network of hydrogel was placed close to the mentioned section. However, because of CARBPOL limitations (max. 8 figures), other figures have not been slit and moved. They would be placed close to their discussions in the proof for publication after manuscript acceptance.

The mechanical property section needs to be improved. The compression test results are not well discussed. In addition, rheological and tensile tests are highly suggested.

Thank you for the comment. The mechanical property section has been improved. Materials were obtained using freeze-drying method in the form of highly porous "sponges" rather than "gels". Therefore, rheological measurements, which are commonly used to characterise gels, are not really applicable here. Furthermore, cylindrical shape of the samples makes it impossible to perform tensile tests. For tissue engineering applications, especially for bone regeneration, compressive strength is an important parameter.

The highlights of the study need to be further emphasized and explicitly discussed. In my opinion, the highlight is the usage of THBA, a benign antioxidant, as the hydrogel crosslinker. However, the manuscript includes too many general discussions (eg. Porous size), impairing the expression of the interesting new discovery.

Thank you for the comment. The highlight (the usage of THBA) has been further discussed.

Reviewer #7

The authors addressed all the comments of the reviewers. I am satisfied with the revision. The paper may be accepted for publication in Carbohydrate Polymers.

Thank you for all your comments that allowed us to improve the manuscript.

Figure 1

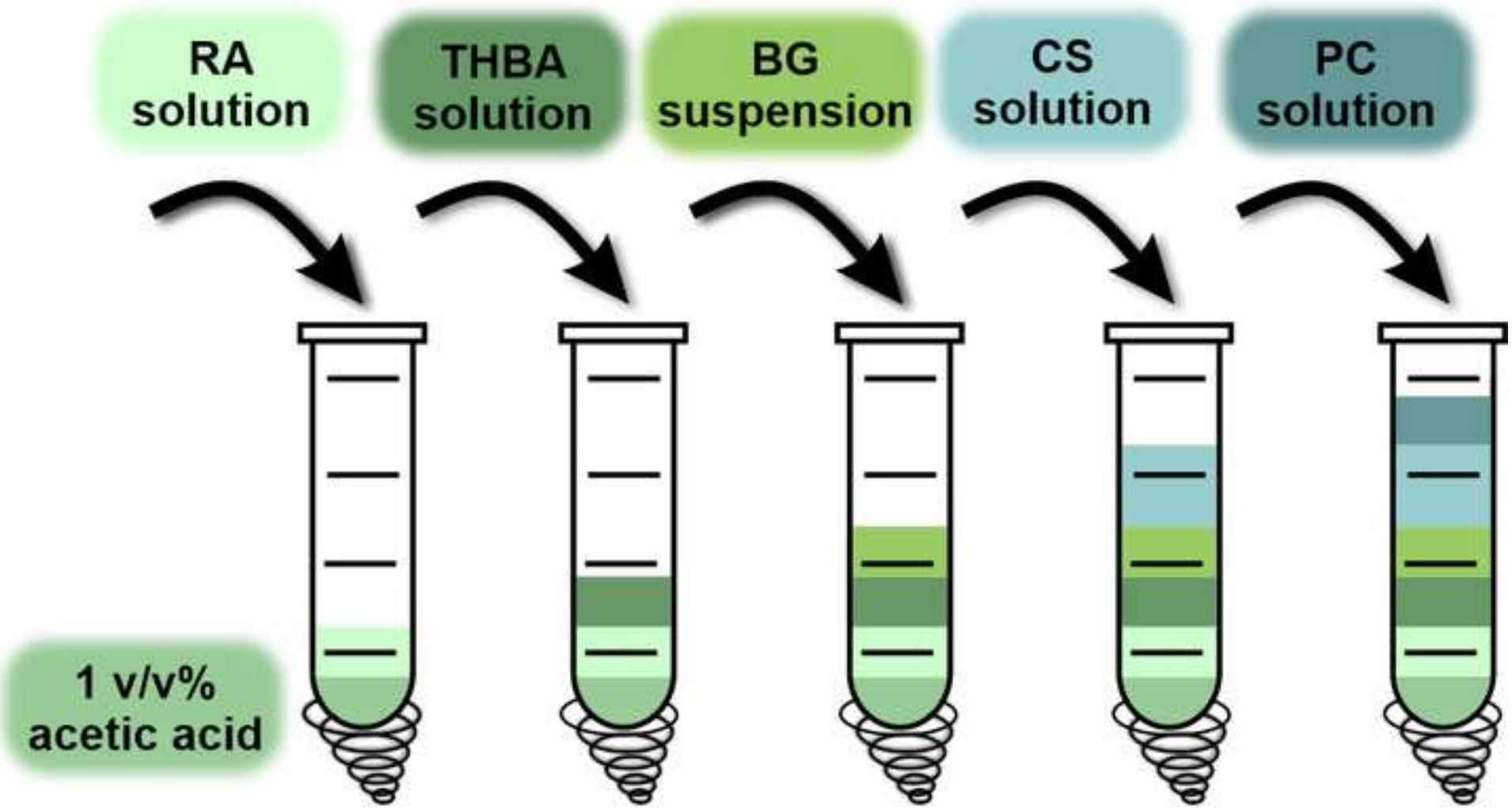

Figure 2

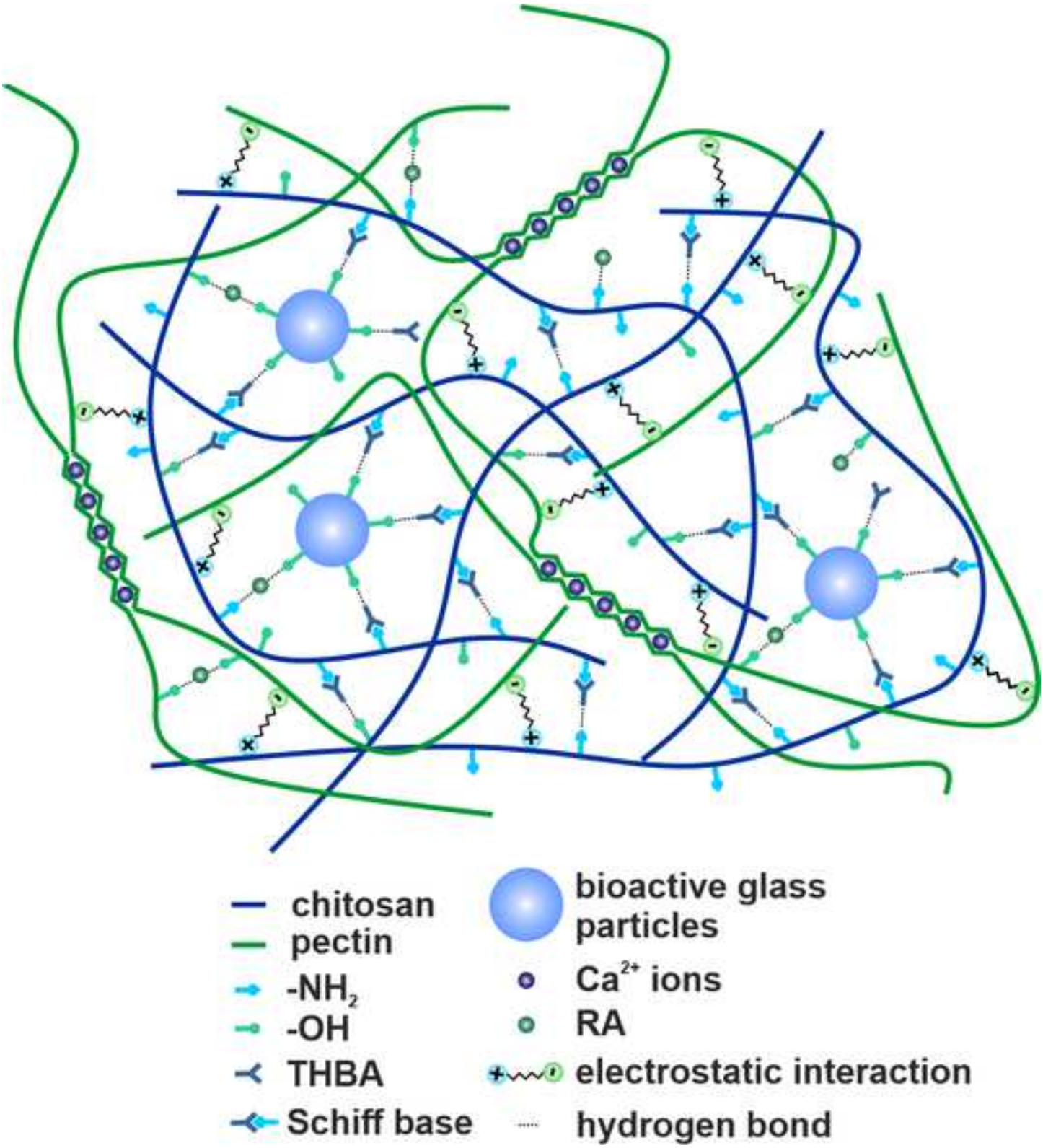

Figure 3

Click here to access/download;Figure(s);FIGURE 3_R3.tif

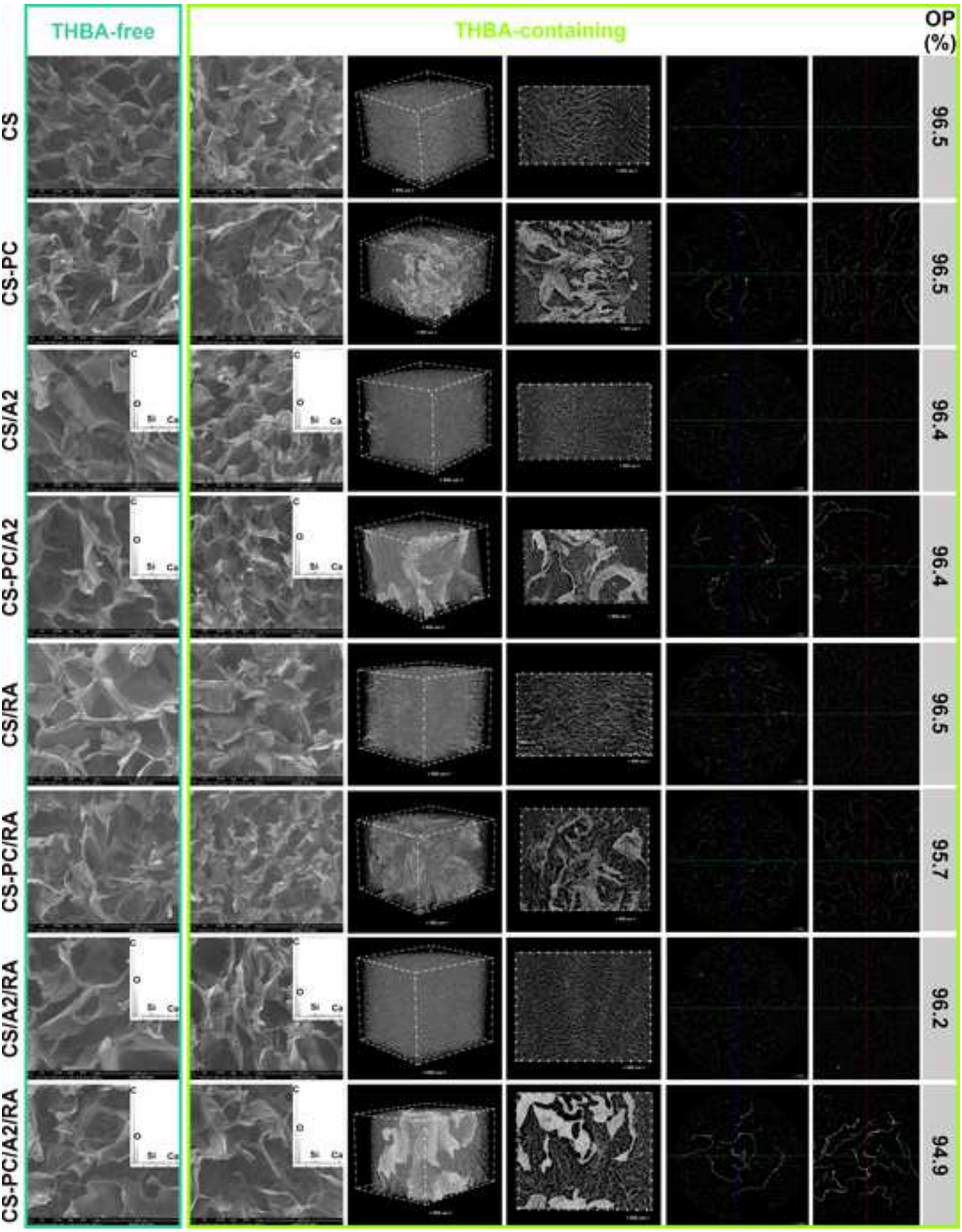

Figure 4

Click here to access/download;Figure(s);FIGURE 4_R3.tif

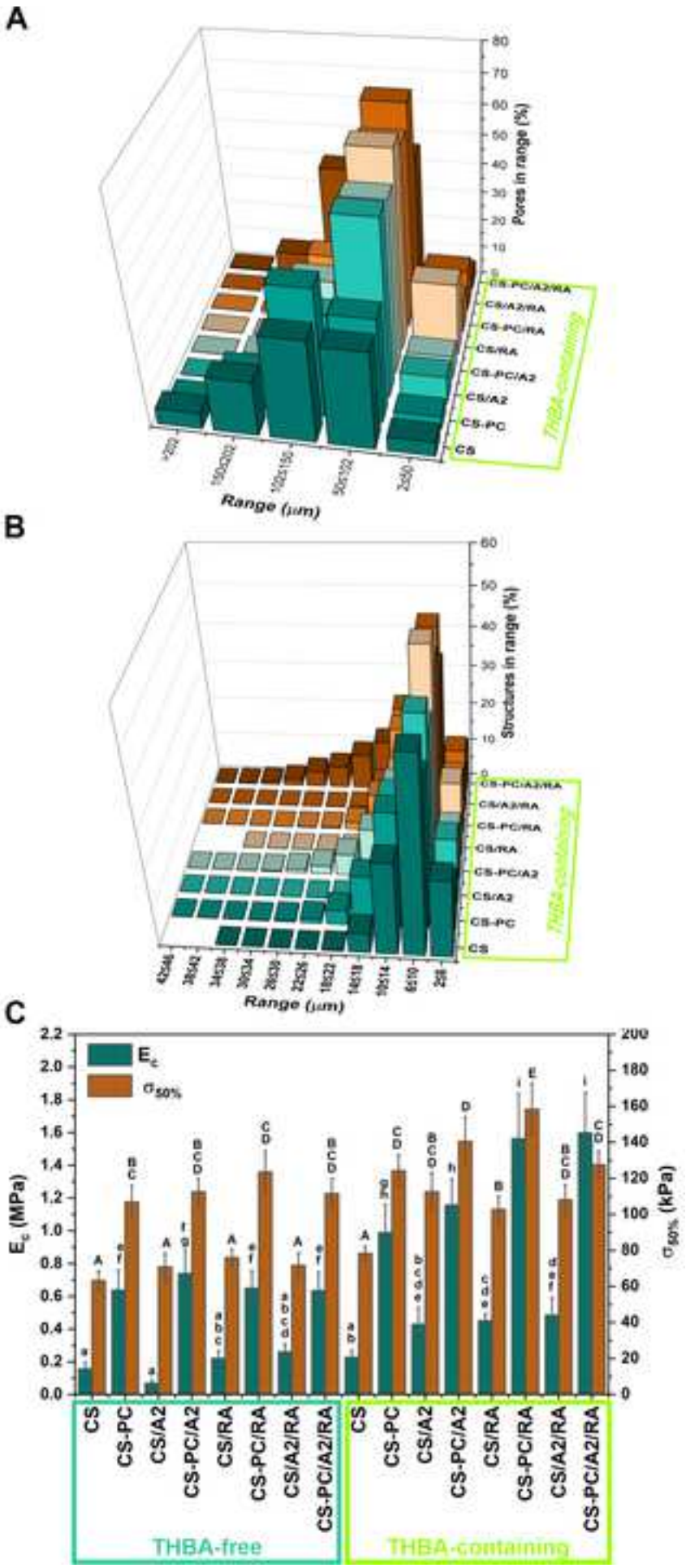

Figure 5

Click here to access/download;Figure(s);FIGURE 5_R3.tif

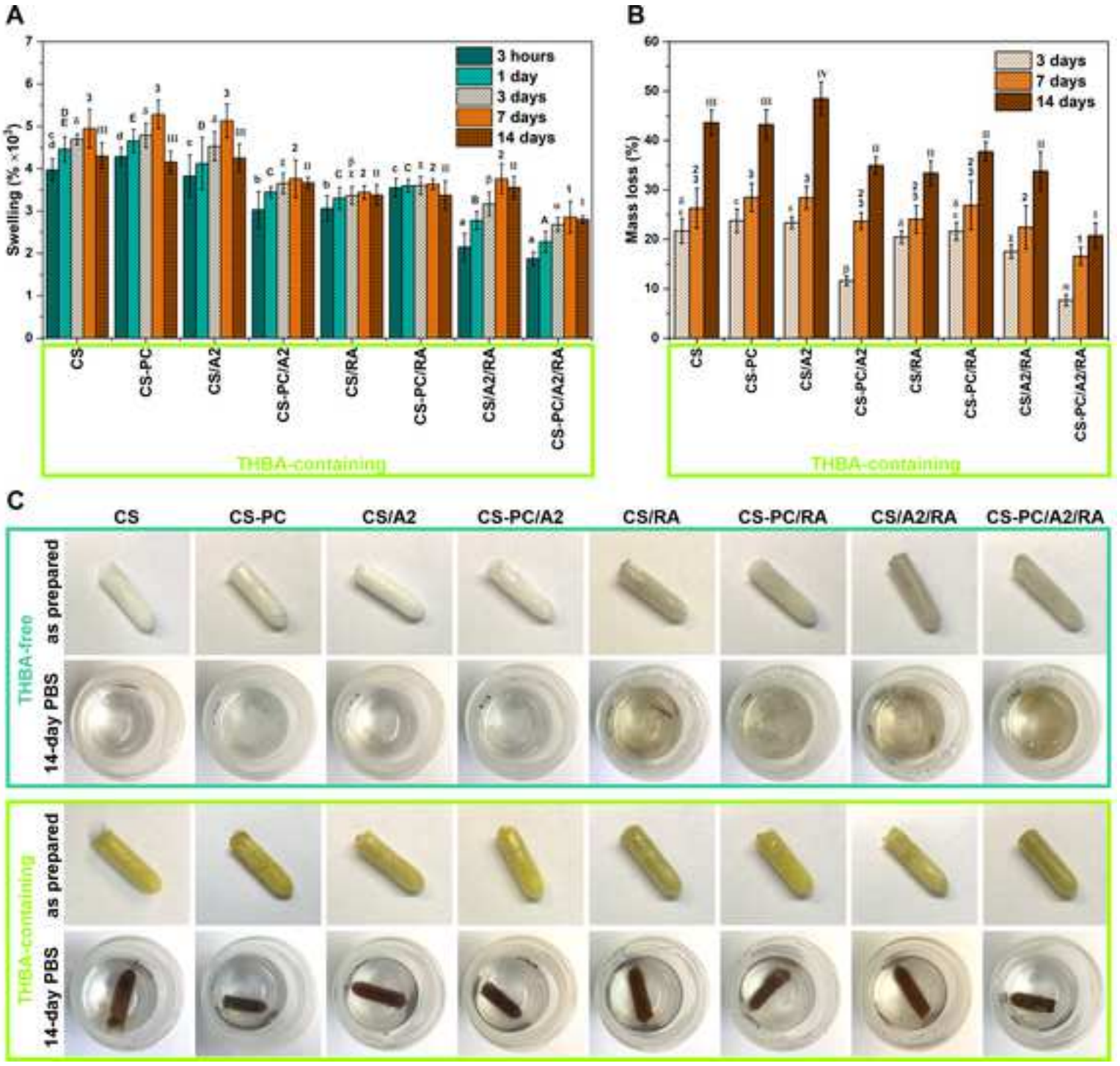

Figure 6

Click here to access/download;Figure(s);FIGURE 6_R3.tif

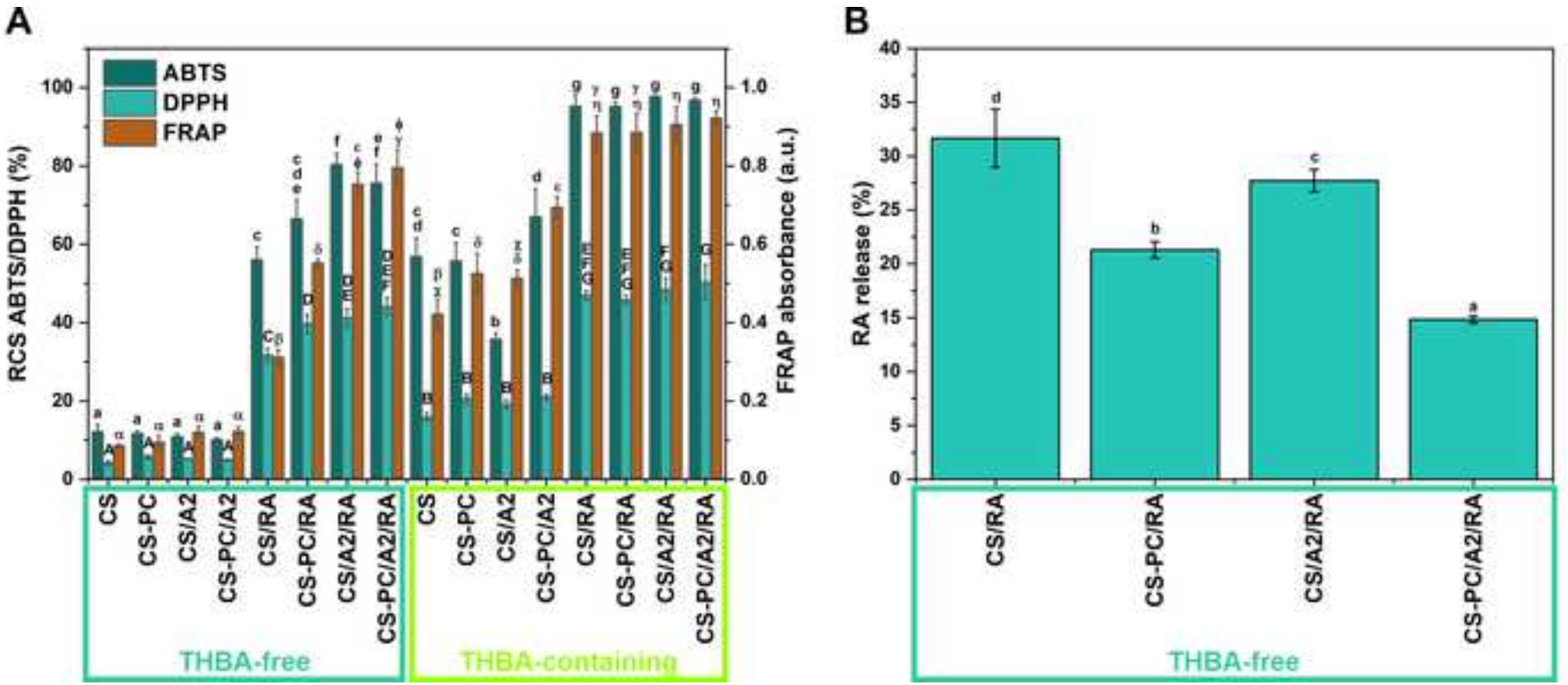

Figure 7

Click here to access/download;Figure(s);FIGURE 7_R3.tif

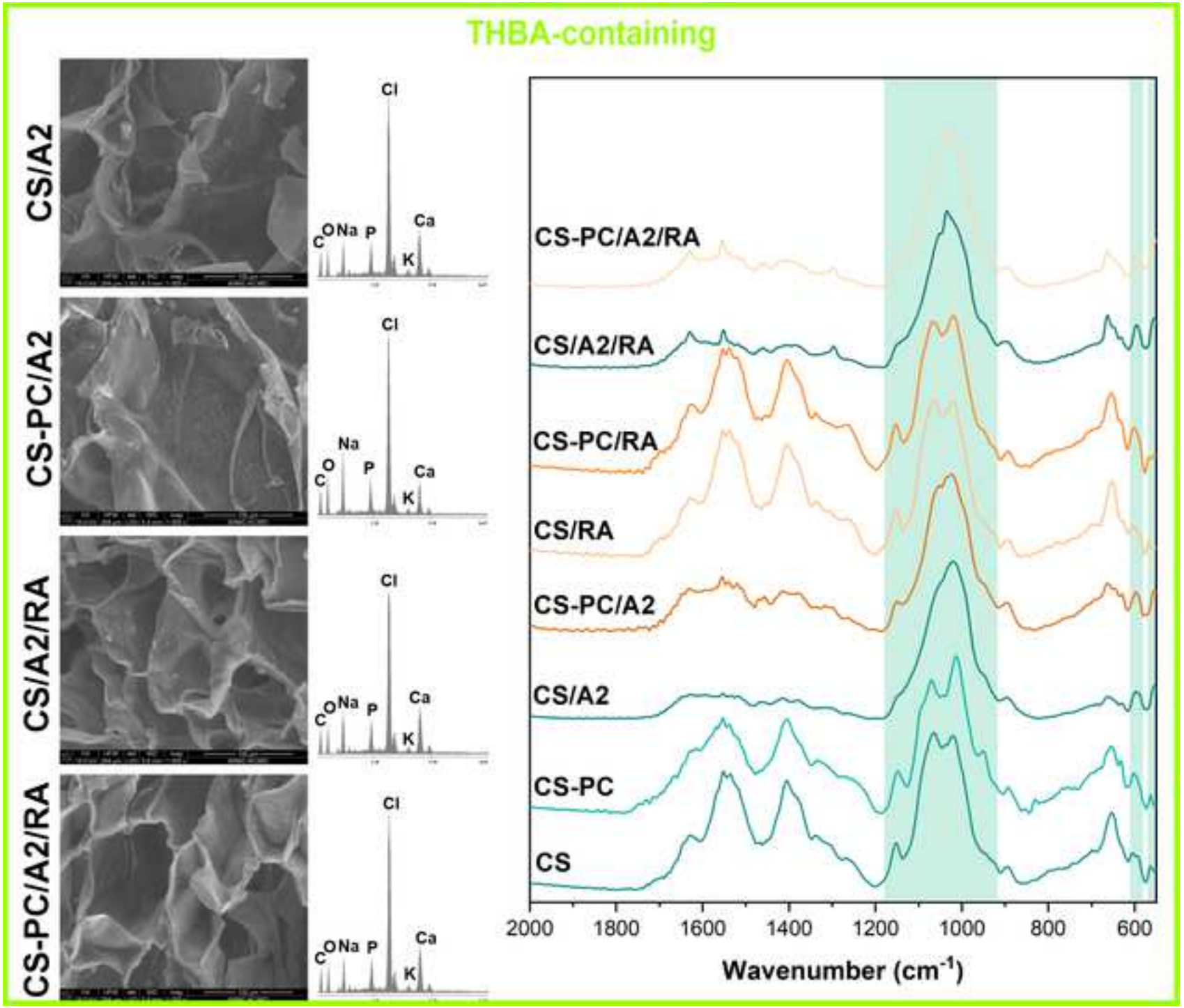

Figure 8

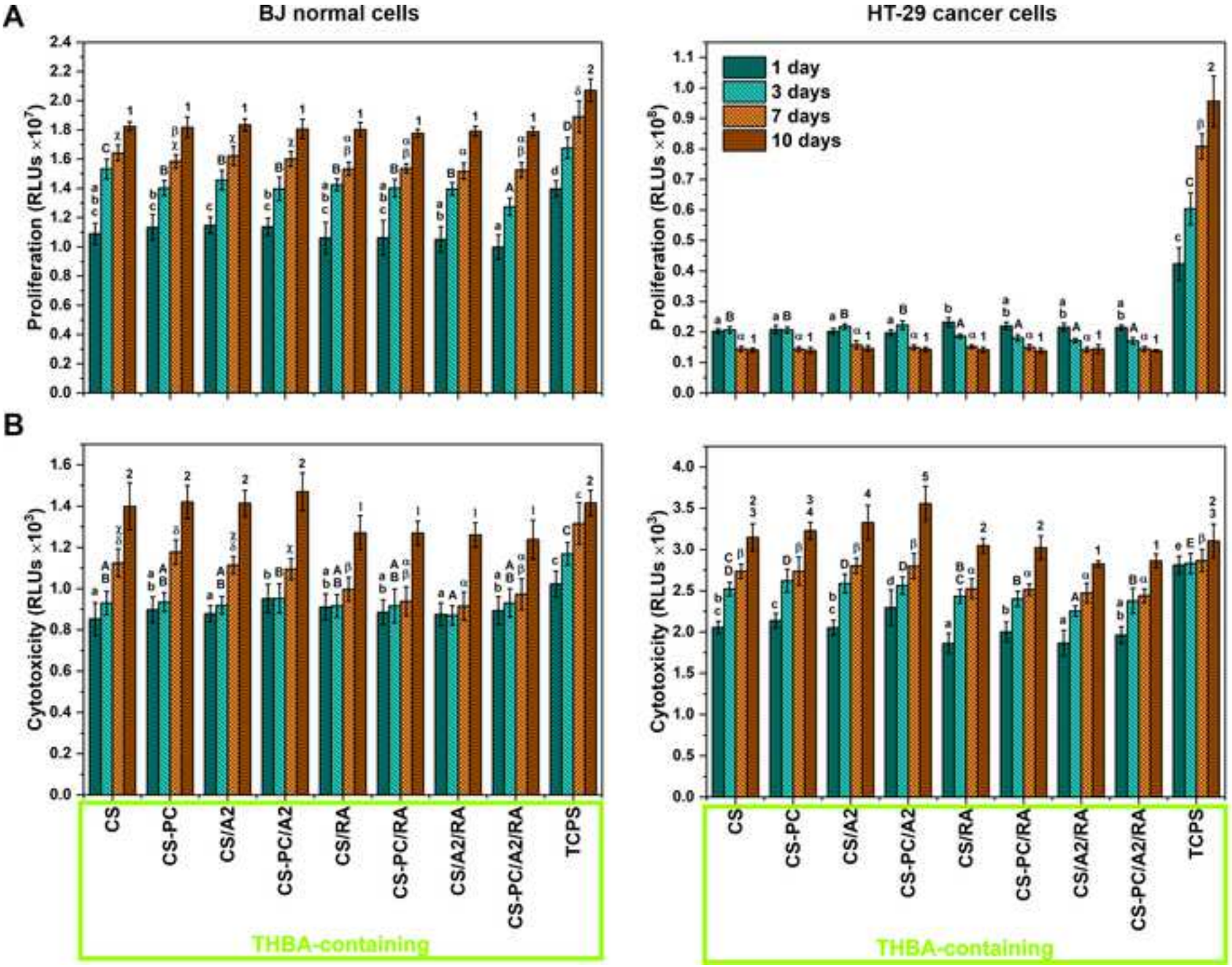

Michal Dziadek – Conceptualization, Methodology, Investigation, Writing - Original Draft, Writing - Review & Editing, Visualization, Supervision, Project administration, Funding acquisition

Kinga Dziadek – Conceptualization, Methodology, Investigation, Visualization, Writing - Original Draft

Szymon Salagierski – Investigation, Visualization, Writing - Original Draft

Mariola Drozdowska – Investigation, Visualization, Writing - Original Draft

Andrada Serafim – Investigation, Visualization, Writing - Original Draft, Funding acquisition

Izabela-Cristina Stancu – Investigation, Visualization, Writing - Original Draft, Funding acquisition

Piotr Szatkowski – Investigation, Visualization, Writing - Original Draft, Funding acquisition

Aneta Kopec – Writing - Review & Editing, Supervision

Izabella Rajzer – Writing - Review & Editing, Supervision

Timothy E. L. Douglas – Writing - Review & Editing, Supervision

Katarzyna Cholewa-Kowalska – Writing - Review & Editing, Supervision, Funding acquisition

Newly crosslinked chitosan- and chitosan-pectin-based hydrogels with high antioxidant and potential anticancer activity

Michal Dziadek [a,b*], Kinga Dziadek [c], Szymon Salagierski [b], Mariola Drozdowska [c], Andrada Serafim [d], Izabela-Cristina Stancu [d], Piotr Szatkowski [e], Aneta Kopec [c], Izabella Rajzer [f], Timothy E. L. Douglas [g,h], Katarzyna Cholewa-Kowalska [b]

[a] Faculty of Chemistry, Jagiellonian University, Krakow, Poland;
[b] Department of Glass Technology and Amorphous Coatings, AGH University of Science and Technology, Krakow, Poland;
[c] Department of Human Nutrition and Dietetics, University of Agriculture in Krakow, Krakow, Poland;
[d] Advanced Polymer Materials Group, University Politehnica of Bucharest, Bucharest, Romania;
[e] Department of Biomaterials and Composites, AGH University of Science and Technology, Krakow, Poland;
[f] Department of Mechanical Engineering Fundamentals, ATH University of Bielsko-Biala, Bielsko-Biała, Poland;
[g] Engineering Department, Lancaster University, Lancaster, United Kingdom;
[h] Materials Science Institute (MSI), Lancaster University, Lancaster, United Kingdom;

*corresponding author: michal.dziadek@uj.edu.pl, dziadek@agh.edu.pl

Abstract

Monoaldehydes, due to natural origin and therapeutic activity, have attracted great attention for their ability to crosslink chitosan hydrogels for biomedical applications. However, most studies have focused on single-component hydrogels. In this work, chitosan-based hydrogels, crosslinked for the first time with 2,3,4-trihydroxybenzaldehyde (THBA), were modified with pectin (PC), bioactive glass (BG), and rosmarinic acid (RA). All of these were not only involved in the crosslinking, but also modulated properties or imparted completely new ones. THBA functioned as a crosslinker, resulting in improved mechanical properties, high swelling capacity and delayed degradation and also imparted high antioxidant activity and antiproliferative effect on cancer cells without cytotoxicity for normal cells. Hydrogels containing PC showed enhanced mechanical strength, while the combination with BG gave improved stability in PBS. All hydrogels modified with BG exhibited the ability to mineralize in SBF. The addition of RA enhanced antioxidant and anticancer activities and promoting the mineralisation process.

Keywords: monoaldehyde; polyelectrolyte complex; bioactive glass; polyphenols; micro-computed tomography

1. Introduction

Hydrogel materials are able to absorb a large amounts of water and swell without dissolving in aqueous media. These unique properties hydrogels owe to three-dimensional crosslinked network of hydrophilic polymer chains. Recently, hydrogels have attracted great attention for their potential application in a wide range of biomedical areas, including tissue engineering and controlled drug delivery systems. This is due to the fact that hydrogels are able to mimic biomechanical characteristics of native extracellular matrix (ECM), providing 3D microenvironments for cell migration, adhesion, and proliferation, as well as promoting the transport of nutrients and signalling molecules. Furthermore, their porosity, high swelling ability, and hydrophilic nature make hydrogels excellent candidates as carriers of hydrophilic biologically active compounds (e.g. drugs, biomolecules, phytochemicals). Generally, all of these properties of hydrogels are highly associated with the degree of crosslinking (Mallick et al., 2020; M. Zhang et al., 2021).

Chitosan (CS), as a glucosamine-based polysaccharide obtained by deacetylation of chitin, is one of the most studied biopolymers in the biomedical applications. CS is characterised by good biocompatibility, biodegradability, inherent antibacterial activity, hemostatic potential, wide availability, and low price (Coimbra et al., 2011). Although CS-based hydrogels for biomedical

applications have been widely studied in recent years, their effective and safe crosslinking still remains a great challenge.

The most frequently used crosslinking agents of CS are dialdehydes, in particular glutaraldehyde (GA). The crosslinking mechanism of dialdehydes, including GA, is based on the formation of imine bonds, well-known as Schiff bases, between two aldehyde groups of GA and amino groups of chitosan chains. However, GA is highly cytotoxic and neurotoxic. In recent years, great interest has been focused on monoaldehydes as CS crosslinking agent, which in many cases, unlike dialdehydes, are naturally occurring compounds with beneficial biological activities (e.g. antioxidant, anticancer, antibacterial) (Iftime et al., 2017; Xu et al., 2018). The crosslinking mechanism of the monoaldehyde is based on imine-bond formation between the single aldehyde group of the monoaldehyde molecule and the amino group of the CS chain accompanied by the hydrophilic/hydrophobic assembling of the CS/aromatic units of the monoaldehyde. The monoaldehyde hydroxyl group in the *ortho* position can form an intramolecular hydrogen bond with the imine nitrogen, providing the stabilization of the imine linkage (Iftime et al., 2017). Furthermore, the hydroxyl groups in other positions can form additional hydrogen bonds with the hydroxyl or the amino groups in chitosan chains, enhancing the crosslinking effect (Xu et al., 2018).

The second important crosslinking mechanism of CS is ionic/electrostatic interaction. Examples of this are polyelectrolyte complexes (PECs), which are formed by electrostatic interactions between cationic amino groups in CS and anionic groups in other polymers, such as carboxyl acid groups of pectin (PC) under specific pH conditions (in the p*K*a range of these two polymers) (Maciel et al., 2015).

PCs are anionic polysaccharides derived mainly from by-products of the fruit processing industry, therefore they are environmentally friendly, available in vast amounts and inexpensive (Neves et al., 2015). PCs show good biocompatibility and biodegradability, as well as a wide range of biological activities, such as anti-inflammatory, antioxidant, and anticancer properties (Cui et al., 2017; Munarin et al., 2011; Neves et al., 2015). PCs, especially low esterified amidated ones, can easily be crosslinked by calcium ions to form hydrogels, also injectable systems (Yuliarti et al., 2017). For these reasons, PCs are receiving increased attention as a hydrogel material for drug delivery and tissue engineering applications (Cui et al., 2017; Douglas et al., 2019; Munarin et al., 2011; Neves et al., 2015).

A combination of CS and PC to obtain PEC hydrogels exploits the biological benefits of both biopolymers while also enabling modification of the material properties, such as mechanical behaviour, wettability, swelling, and degradation (Chen et al., 2010; Coimbra et al., 2011).

CS/PC-based hydrogels showed high cytocompatibility with many cell types (Birch et al., 2015; Li et al., 2010), capacity to be loaded with drugs (Luppi et al., 2010; Neufeld & Bianco-Peled, 2017) and natural biological active compounds (Maciel et al., 2015), indicating high potential in biomedical applications.

In order to improve the biological and physicochemical properties of hydrogels or impart completely new functionalities to them, various additives are used. One of them is bioactive ceramic, especially bioactive glass (BG). BGs have significantly altered the properties of hydrogels relevant for bone regeneration applications (mechanical properties, microstructural/topographical features, osteoblast activity) (Dziadek, Charuza, et al., 2021). Furthermore, calcium phosphate (CaP) forming ability of BGs and osteogenic properties of their dissolution products (i.a. silica, calcium ions) have induced hydrogel mineralization with a CaP phase, assuring improved mechanical properties, direct chemical bonding with bone, and stimulation of bone regeneration (Sitarz et al., 2013; Wajda et al., 2016, 2018). Other additives used in hydrogels are biologically active compounds. In recent years, much attention has been paid to naturally occurring chemicals - polyphenols, as alternative for drugs and biomolecules. This is due to the multiple biological activities of polyphenols, such as antioxidant, anticancer, anti-inflammatory, antimicrobial and osteostimulation properties, and minor side effects (Dziadek, Dziadek, et al., 2021). One of the polyphenols frequently found in herbal plants is rosmarinic acid (RA). RA has exhibited multi-faceted activity, for instance strong antioxidant, anticancer, and anti-inflammatory activities (Kuhlmann & Röhl, 2008; Xavier et al., 2009). Furthermore, RA has been shown to regulate bone metabolism by inducing osteoblast differentiation and inhibiting osteoclast activity (Lee et al., 2015).

As we have shown in previous work, calcium-rich sol-gel-derived BG particles can be a sufficient rich source of Ca^{2+} ions for internal crosslinking of low esterified amidated PC (Douglas et al., 2019). Furthermore, numerous silanol groups (Si-OH) of sol-gel-derived BG and hydroxyl groups of polyphenolic compounds may interact with each other and also with functional moieties of chitosan (-OH, $-NH_2$) and pectin (-OH, -COOH) to form hydrogen bonds (Douglas et al., 2017; Dziadek, Dziadek, et al., 2021; Hu et al., 2021).

In this work, the phenolic monoaldehyde - 2,3,4-trihydroxybenzaldehyde (THBA) was used for the first time as a crosslinking agent in CS-based hydrogels for potential use in tissue engineering applications. It was hypothesize that the use of a second hydrogel-forming polymer, namely PC, as well as different functional additives, including calcium-rich sol-gel-derived BG particles and polyphenolic compounds (RA) would significantly affect the crosslinking process, and therefore the properties of CS-based hydrogels. A series of highly porous scaffolds was

evaluated in terms of (i) microstructure and porosity; (ii) mechanical properties; (iii) thermal properties; (iv) swelling and degradation behaviour; (v) the *in vitro* mineralisation process; (vi) antioxidant activity; (vii) *in vitro* cytotoxicity and antiproliferative activity against normal and cancer human cells.

2. Materials and methods

2.1. Preparation of the materials

Bioactive glass powder of the following composition (%mol) 54CaO-40SiO_2-6P_2O_5, denoted as A2, was synthetized using a sol-gel technique as reported previously (Zagrajczuk et al., 2017). BG was milled in an attritor with ZrO_2 balls in isopropyl alcohol medium to obtain a powder with a particle size of 1 μm (d_{50}). The particle size distribution and SEM image of BG are shown in **Fig. A.1**. Particle size distribution was measured by laser diffraction Mastersizer-S equipment (Malvern Instruments, UK) as described previously (Douglas et al., 2019).

Hydrogels were prepared using freeze-drying process. Chitosan (medium molecular weight; 75-85% deacetylated; Sigma-Aldrich, Germany) and pectin (low esterified amidated pectin from citrus peels; degree of esterification - 27.4%, degree of amidation - 22.8%, galacturonic acid content - 93.5%; Herbstreith & Fox, Germany) solutions (2 w/v%) were prepared by dissolving CS and PC powders in 1 v/v% acetic acid aqueous solution and deionised water, respectively. The pH values of the polymer solutions were 4.5 and 4.4, respectively. 2,3,4-trihydroxybenzaldehyde (Sigma-Aldrich, Germany) was used as crosslinking agent. Materials with and without THBA were prepared. THBA, rosmarinic acid (Carbosynth Ltd, UK), and BG powder was introduced into materials in the form of 1 w/v% solution/suspension in deionised water. Adequate solutions/suspensions (CS/PC/THBA/RA/BG) were mixed (3000 rpm) at room temperature in 2-mL Eppendorf tubes using a vortexer to obtain materials of compositions presented in **Table 1**. All mixtures were filled up to constant volume using 1 v/v% acetic acid. The scheme showing the order of mixing of the components is shown in **Fig. 1A** (if a particular component was not added, the respective mixing step for that component was omitted). The samples in Eppendorf tubes were frozen in a laboratory freezer at -24 ℃ for 48 h and then freeze-dried (Alpha 1–4 LSCplus, Christ, Germany, ice condenser temperature -55 °C, vacuum 0.1 mbar) for 48 h.

Table 1. The compositions of materials.

Material	CS (w/w%)	PC (w/w%)	THBA (w/w%)	RA (w/w%)	A2 BG (w/w%)
Uncrosslinked materials					
CS	100	-	-	-	-
CS-PC	70	30	-	-	-
CS/A2	100	-	-	-	5
CS-PC/A2	70	30	-	-	5
CS/RA	100	-	-	2	-
CS-PC/RA	70	30	-	2	-
CS/A2/RA	100	-	-	2	5
CS-PC/A2/RA	70	30	-	2	5
Crosslinked materials					
CS	100	-	2	-	-
CS-PC	70	30	2	-	-
CS/A2	100	-	2	-	5
CS-PC/A2	70	30	2	-	5
CS/RA	100	-	2	2	-
CS-PC/RA	70	30	2	2	-
CS/A2/RA	100	-	2	2	5
CS-PC/A2/RA	70	30	2	2	5

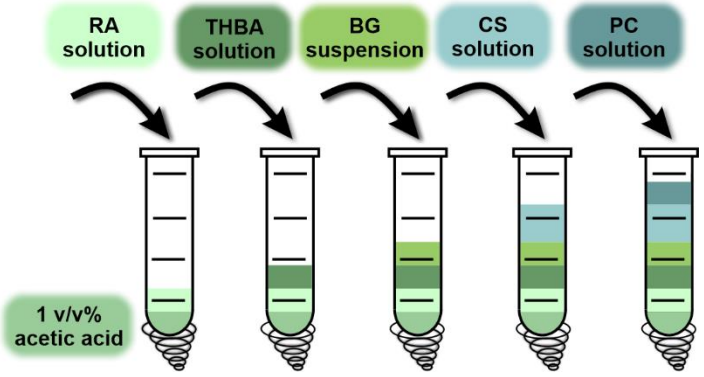

Figure 1. Scheme showing the order of mixing of the components (if a particular component was not added, the mixing step for that component was omitted).

2.2. Microstructure analysis

THBA-free and THBA-containing hydrogels were analysed using ultra-high resolution scanning electron microscope (SEM) equipped with a field emission gun and a secondary electron detector (Nova NanoSEM 200 FEI Europe Company, accelerating voltage 10-15 kV, spot 4) coupled with an energy dispersion X-ray (EDX) analyser with a SiLi detector (EDAX, Netherlands) in the low vacuum mode. Cross sections were prepared by hydrogel cutting with a scalpel blade. Materials were analysed after coating with a carbon layer.

Architecture of crosslinked hydrogels were evaluated using micro-computed tomography (µ-CT) using a SkyScan 1272 equipment high-resolution X-ray microtomograph (Bruker Micro-CT, Belgium). 2D projections were registered averaging 3 frames, rotation of 0.3° and 800 ms exposure time. The images were registered at a resolution of 4904 x 3280 at an accelerating voltage of 50 kV and a beam current of 200 µA. The pixel size was fixed at 2 µm.

2.3. Mechanical analysis

Mechanical strength of the hydrogels was determined using an Inspekt 5 Table Blue testing machine (Hegewald & Peschke, Germany) equipped with a 100 N load cell. Samples were cut into cylinders of 10 mm height and compressed with a displacement rate of 5 mm min^{-1} (n = 10). Subsequently, Young's modulus (E_C) and the stresses corresponding to compression of a sample by 50% ($\sigma_{50\%}$) were measured. The results were expressed as mean ± standard deviation (SD).

2.4. Thermal analysis

Thermogravimetric analysis (TGA) was performed using a Discovery TGA 550 analyser (TA Instruments, USA) in the temperature range from 40 to 600 °C at a heating rate of 10 °C min^{-1}, under a nitrogen atmosphere. The samples (c.a. 15 mg) were placed in a platinum crucible.

2.5. FTIR analysis

The attenuated total reflection Fourier transform infrared (ATR-FTIR) spectra were registered using Vertex 70v spectrometer (Bruker, USA) equipped with a ZnSe ATR crystal. Spectra were collected in the 550-4000 cm^{-1} spectral range with a resolution of 4 cm^{-1} and by averaging 128 scans.

2.6. XPS analysis

X-ray photoelectron spectroscopy (XPS) analysis was performed in an ultrahigh vacuum system ($5 \cdot 10^{-9}$ mbar) equipped with an SES R4000 analyser (Gammadata Scienta, Sweden).

A monochromatic Al Kα X-ray source (1486.6 eV) was used. The electron binding energy of C1s peak was referenced at 284.8 eV. The obtained XPS spectra were analysed using CasaXPS 2.3.15 software.

2.7. Swelling and degradation studies

Swelling and degradation behaviour of hydrogels was investigated by incubating the samples (n = 5) in phosphate buffered saline (PBS, pH 7.4) at 37 °C. For swelling tests, the samples were weighed at the beginning of the experiment and again after 3 h, 1, 3, 7, and 14 days of incubation. Before weighing the samples were placed on filter paper to remove excess PBS from the surface. Swelling of each sample was calculated as follows: $\frac{W_t - W_0}{W_0} \times 100\%$, where W_t is weight after specific period of incubation, W_0 is weight before incubation. For degradation tests, the samples were weighed at the beginning of the experiment and again after 3, 7, and 14 days of incubation after freeze-drying. Mass loss of each sample was calculated as follows: $\frac{W_0 - W_t}{W_0} \times 100\%$, where W_0 is the weight of the sample before incubation and W_t is the weight of the freeze-dried sample after a specific period of incubation. The results were expressed as mean ± standard deviation (SD).

2.8. Antioxidant activity and release of THBA and RA

Antioxidant activity of the hydrogels was evaluated using ABTS and DPPH free radical scavenging assays and ferric reducing antioxidant power (FRAP) test (Dziadek, Dziadek, et al., 2021). The samples were incubated with shaking in ABTS, DPPH, and FRAP working solutions for 10 minutes in the dark at 30 ºC (n = 3). For ABTS, DPPH, and FRAP assays, the changes of absorbance at 734 nm, 515 nm, and 593 nm respectively, were measured using a spectrometer (UV-1800, RayLeigh, China). The radical scavenging capacity (RSC) of the materials was calculated as follows: $RSC = \frac{A_0 - A_S}{A_0} \times 100\%$, where A_S was the absorbance of the solution after sample incubation, and A_0 was the absorbance of ABTS and DPPH working solutions. The results of the FRAP test were expressed as absorbance. The results were expressed as mean ± standard deviation (SD).

The release of THBA and RA from hydrogels to PBS was evaluated using HPLC. A Prominence-i LC-2030C 3D Plus system (Shimadzu, Japan) equipped with a diode array detector (DAD) was used. The separation was performed on the Luna Omega 5 µm Polar C18, 100 A, 250 x 10 mm column (Phenomenex, California, USA) at 40ºC. The mobile phase was a mixture of two eluents: A – 0.1 % v/v formic acid in UHQ water and B – 0.1 % v/v formic acid in methanol. The flow rate of the mobile phase was 1.2 mL min^{-1}. The analysis was carried out

with the following gradient conditions: from 20% to 40% B in 10 min, 40% B for 10 min, from 40% to 50% B in 10 min, from 50% to 60% B in 5 min, 60% B for 5 min, from 60% to 70% B in 5 min, from 70% to 90% B in 5 min, 90% B for 5 min, from 90% to 20% B (the initial condition) in 1 min and 20% B for 4 min, resulting in a total run time of 60 min. The injection volume was 20 μL. All of the reagents used for HPLC analysis were purchased from Sigma-Aldrich, Germany.

2.9. *In vitro* mineralisation studies

The mineralization process of hydrogels was performed by incubation in simulated body fluid (SBF), prepared according to Kokubo and Takadama (Kokubo & Takadama, 2006). Samples were incubated in SBF for 7 and 14 days at 37 ℃, freeze-dried and analysed using SEM/EDX and ATR-FTIR methods as mentioned above.

2.10. *In vitro* cell studies

The human normal skin fibroblasts (BJ, ATCC, USA) and the human colon cancer epithelial cells (HT-29, ATCC, USA) were cultured in direct contact with crosslinked materials in Eagle's Minimum Essential Medium (EMEM, Sigma-Aldrich, MO, USA) and McCoy's 5a Medium Modified (ATCC, USA), respectively, both containing 10% Fetal Bovine Serum (FBS) at a density of $2 \cdot 10^4$ cells/mL/well for 1, 3, 7, and 10 days in 48-well plates. The bottom surfaces of tissue culture polystyrene (TCPS) wells served as a control. The proliferation rate of cells and cytotoxicity of hydrogels were assessed using the ToxiLight™ BioAssay Kit and ToxiLight™ 100% Lysis Reagent Set (Lonza, USA) according to the manufacturer's protocol. The kit was used to quantify adenylate kinase in both supernatant (representing damaged cells) and lysate (representing intact adherent cells). The results were expressed as mean ± standard deviation (SD) from 4 samples for each experimental group.

2.11. Statistical analysis

The results were analyzed using one-way analysis of variance (ANOVA) with Duncan post hoc tests, which were performed with Statistica 13 (StatSoft®, USA) software. The results were considered statistically significant when $p<0.05$.

3. Results and discussion

The use of monoaldehydes as crosslinking agents of chitosan is not as common as the use of other ones, e.g. glutaraldehyde. However, due to their natural origin, low cytotoxicity, low costs, and therapeutic activity, they have attracted great attention for crosslinking chitosan hydrogels for biomedical applications. To date, the following monoaldehydes have been used - vanillin (Hu et al., 2021; Karakurt et al., 2021; Xu et al., 2018), salicylaldehyde (Iftime et al.,

2017, 2020), nitrosalicylaldehyde (Craciun et al., 2019; Olaru et al., 2018), and cinnamaldehyde (Marin et al., 2014). In most cases, single-component hydrogels were obtained. However, there are only a few reports on the introduction of functional components into imine-chitosan hydrogels and examination of their effect on the crosslinking process, and thus the final properties of materials. In recent works, melt-derived bioactive glass particles (Hu et al., 2021) and diclofenac sodium salt (Craciun et al., 2019; Iftime et al., 2020), as a model drug, were used. In the present study we developed multicomponent chitosan-based hydrogels modified with a second hydrogel-forming polymer - pectin, as well as different functional additives – bioactive glass particles and rosmarinic acid. For systematic evaluation of the obtained hydrogels, the additives were introduced alone or in combination to both materials prepared in the presence and absence of monoaldehyde (THBA, pyrogallolaldehyde). It is worth mentioning that the THBA molecule contains three hydroxyl groups which, in addition to their ability to stabilize the imine bond, provided additional binding sides for the chains of both polymers and other components. Importantly, these three hydroxyl groups impart antioxidant properties to the THBA. Pectin was able to form polyelectrolyte complexes with chitosan through electrostatic interactions between ionised moieties. The BG particles used, similarly to RA, also contain numerous hydroxyl groups capable of forming hydrogen bonds. Furthermore, calcium ions, massively released from BG particles, were involved in ionic crosslinking of pectin. All of these reactions and interactions provided a multi-level crosslinking effect of chitosan-based hydrogels, as was schematically illustrated in **Fig. 2**, affecting their properties discussed in the next subsections.

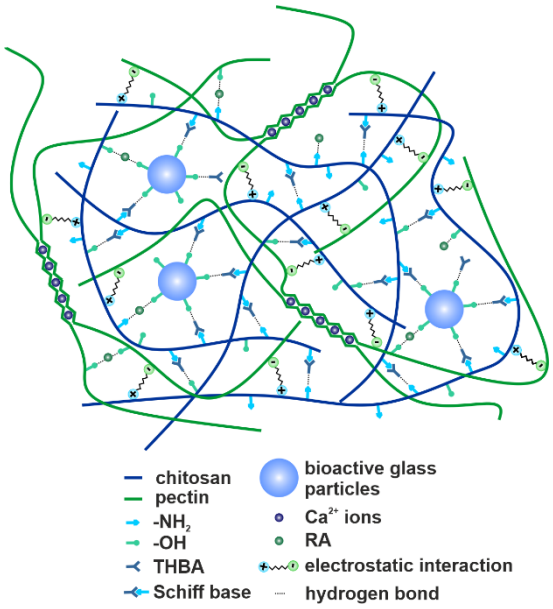

Figure 2. Schematic illustration of the network of THBA-containing CS-PC/A2/RA hydrogel.

3.1. Microstructure analysis

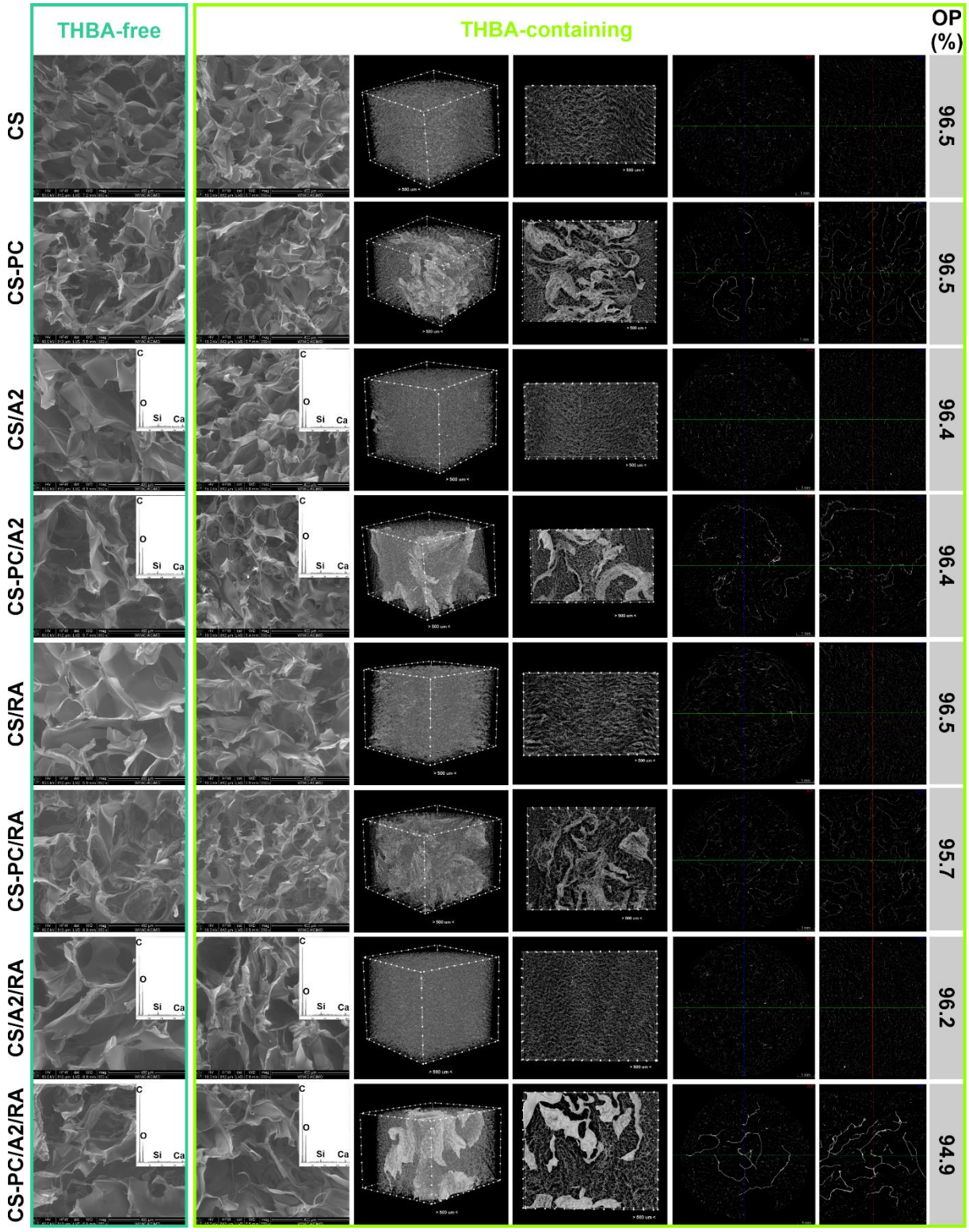

Figure 3. Representative SEM images and EDX spectra of the THBA-free and THBA-containing hydrogels. Representative μCT analyses of the crosslinked hydrogels - 3D reconstructions, cross sections, and open porosity (OP).

SEM analysis of hydrogels revealed irregular highly porous morphology characteristic of biopolymer-based porous materials obtained using freeze-drying processes (**Fig. 3**) (Coimbra et al., 2011; Luppi et al., 2010). All materials showed sheet/sponge-like structures. Additionally, the hydrogels with pectin contained fibrous-like structures, observed also by Coimbra et al., 2011 and Luppi et al., 2010 in CS-PC porous materials. Pores of crosslinked materials seemed be smaller compared to uncrosslinked hydrogels. This may be due to lower amounts of water entrapped between crosslinked chitosan chains (Iftime et al., 2017), which was confirmed by TG analysis (**Fig. A.4**). Although BG particles are not clearly visible in SEM and µCT analyses, the main components of BG (Si, Ca) were detected using EDX analysis, confirming their presence in the hydrogel matrices. This may be related to the low concentration of BG particles in materials (5 w/w%) and their highly homogeneous distribution with no tendency to agglomerate.

µCT analysis of crosslinked hydrogels proved nearly 100% interconnectivity of the pores and high porosity, regardless of the composition of the hydrogels. Open porosity was in the range of 94.9% – 96.5% (**Fig. 3**). The analysis of pore size distribution showed that all hydrogels had pores predominantly in the range of 50-150 µm (**Fig. 4A**), which is consistent with SEM observations (**Fig. 3**). Smaller (2-50 µm) and larger (>150 µm) pores were also present, as depicted by **Fig. 4A**. Such multi-scale pore size distribution, high porosity and interconnectivity promote migration and proliferation of osteogenic cells, vascularization, transport of nutrients and waste, as well as bone tissue ingrowth (Iviglia et al., 2016). Wall thickness was predominantly in the range of 2-18 µm (**Fig. 4B**). 3D reconstructions and cross sections obtained from µCT analysis revealed that CS-based materials had homogenous porous morphology. In the case of CS-PC-based hydrogels, two phases differing in microstructure were observed. Within the most porous phase, similar to that observed in CS-based materials, an inhomogenously distributed and significantly less porous second phase was noted. The latter was possibly PC and/or PC-CS PEC. Inhomogeneous distribution of the PC-containing phase probably results from immediate electrostatic interactions between pectin and chitosan during material preparation. This may also explain the lack of aforementioned agglomeration of BG. This was in contrast to our previous observations made for injectable PC/BG hydrogels, in which non-uniformly distributed agglomerates of A2 BG particles were noted, as a result of extremely rapid local crosslinking process of pectin induced by Ca^{2+} ions released from BG (Douglas et al., 2019). It should be pointed out that during hydrogel preparation, PC solution was added after mixing BG suspension with chitosan solution. As both calcium-induced

crosslinking of pectin and formation of PEC are competitive processes, the order in which the components were mixed favours the latter process, preventing BG agglomeration.

To date, μCT techniques have been used to investigate hydrogel microstructure and distribution of inorganic particles in hydrogel matrices (Douglas et al., 2019; Dziadek, Charuza, et al., 2021; Dziadek et al., 2019). However, our results clearly indicate that μCT imaging is also useful tool to study homogeneity and interactions in hydrogel polyelectrolyte complex matrices formed between polyanions and polycations, i.e. chitosan and pectin.

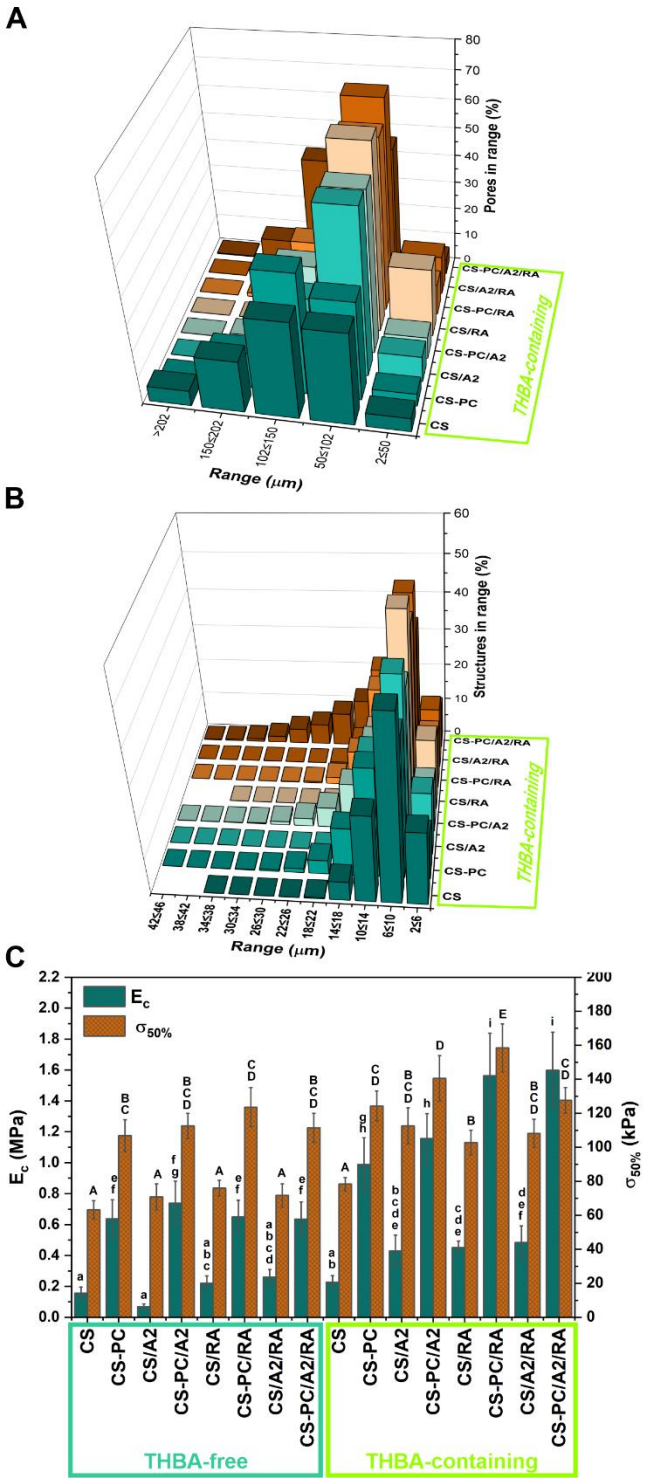

Figure 4. Quantitative data based on μCT analyses of the THBA-containing hydrogels: pore size distribution (A) and structure size distribution (B). Compression test results: Young's modulus and stresses corresponding to compression of a sample by 50% of the THBA-free and THBA-containing hydrogels (C). Statistically significant differences ($p < 0.05$) between materials are indicated by subsequent lower (E_C) and upper ($\sigma_{50\%}$) Latin letters. Different letters indicate statistically significant differences.

3.2. Mechanical analysis

As shown in **Fig. 4C**, hydrogels crosslinked with THBA exhibited significantly higher values of E_c and $\sigma_{50\%}$ (0.22-1.60 MPa and 78-158 kPa, respectively) compared to materials without THBA (0.07-0.73 MPa and 63-123 kPa, respectively). In turn, the presence of pectin in both THBA-containing and THBA-free materials led to significant increases in E_c and $\sigma_{50\%}$ (0.64-1.60 MPa and 106-158 kPa, respectively), when comparing to materials without PC (0.07-0.48 MPa and 63-113 kPa, respectively). Interestingly, improved mechanical properties were observed despite an uneven distribution of the PC-containing phase. However, because of its lower porosity, this phase may be considered as a reinforcing element of a highly porous hydrogel matrix. In the group of materials crosslinked with THBA, the presence of each additive resulted in higher values of both parameters tested. However, the highest E_c values were showed by CS-PC-based hydrogels modified with RA (CS-PC/RA, 1.56 MPa) as well as with both RA and BG (CS-PC/A2/RA, 1.60 MPa), while the highest $\sigma_{50\%}$ value was noted for the first mentioned one (CS-PC/RA, 158 kPa).

Crosslinking has been shown to be an effective strategy to enhance the mechanical properties of biopolymers as a result of formation of a three-dimensional polymer network (Martínez et al., 2015). Xu et al., 2018 showed that the formation of Schiff base bond/hydrogen bond linkage in chitosan hydrogels crosslinked with vanillin provide good mechanical strength and additional self-healing properties. The effect of interactions occurring between chitosan and pectin chains (electrostatic, ion-dipole interactions and hydrogen bonding) on improvement of mechanical properties of porous CS/PC materials was previously observed (Demir et al., 2020). In turn, Chen et al., 2010 showed that the presence of Ca^{2+} ions in a CS-PC PEC membrane significantly improved its tensile strength, because of additional calcium-mediated ionic interactions between pectin chains. In recent work, BG particles were considered as a co-crosslinker, improving mechanical behaviour of CS/BG/vanillin hydrogels. BG particles provided additional binding sites between chitosan and vanillin through multiple hydrogen bonding (Hu et al., 2021). Taking together, the improved mechanical properties of the obtained multicomponent scaffolds could be attributed to the higher crosslinking degree promoted by multifaceted interactions between components.

Formation of the Schiff base in the chitosan matrix was confirmed by development of a distinct yellow colour (**Fig. 5C**) (Stroescu et al., 2015). The FTIR spectra of THBS-containing hydrogels showed an absorption band at 1628 cm^{-1}, which may be attributed to the stretching vibration of imine bonding (**Fig. A.2**). Furthermore, an absorption band of the phenolic hydroxyl groups of THBA shifted from 1279 to 1268 cm^{-1}, which may be due to the H-bonding

between THBA and other components (Y. Zhang et al., 2014). The high-resolution C1s and N1s XPS spectra of the THBA-containing CS hydrogel revealed peaks at 288.8 eV and 398.8 eV (**Fig. A.3**), respectively, which can be assigned to the binding energy of the C=N bond (Gao et al., 2021), suggesting that a Schiff base reaction occurred. When analysing the TG curves, crosslinked materials showed lower water content (lower initial weight loss up to 200 ℃) as well as enhanced thermal stability (higher temperature of thermal decomposition, occurring between 200 and 350 ℃, and higher residual weight) compared to uncrosslinked hydrogels, confirming the presence of covalent Schiff base bonding (**Fig. A.4**) (Montaser et al., 2019). Moreover, in the case of uncrosslinked materials, temperature of thermal decomposition of CS-PC hydrogels tended to be higher compared to CS materials, which may indicate ionic interactions between both polymers (Martins et al., 2018).

3.3. Swelling and degradation studies

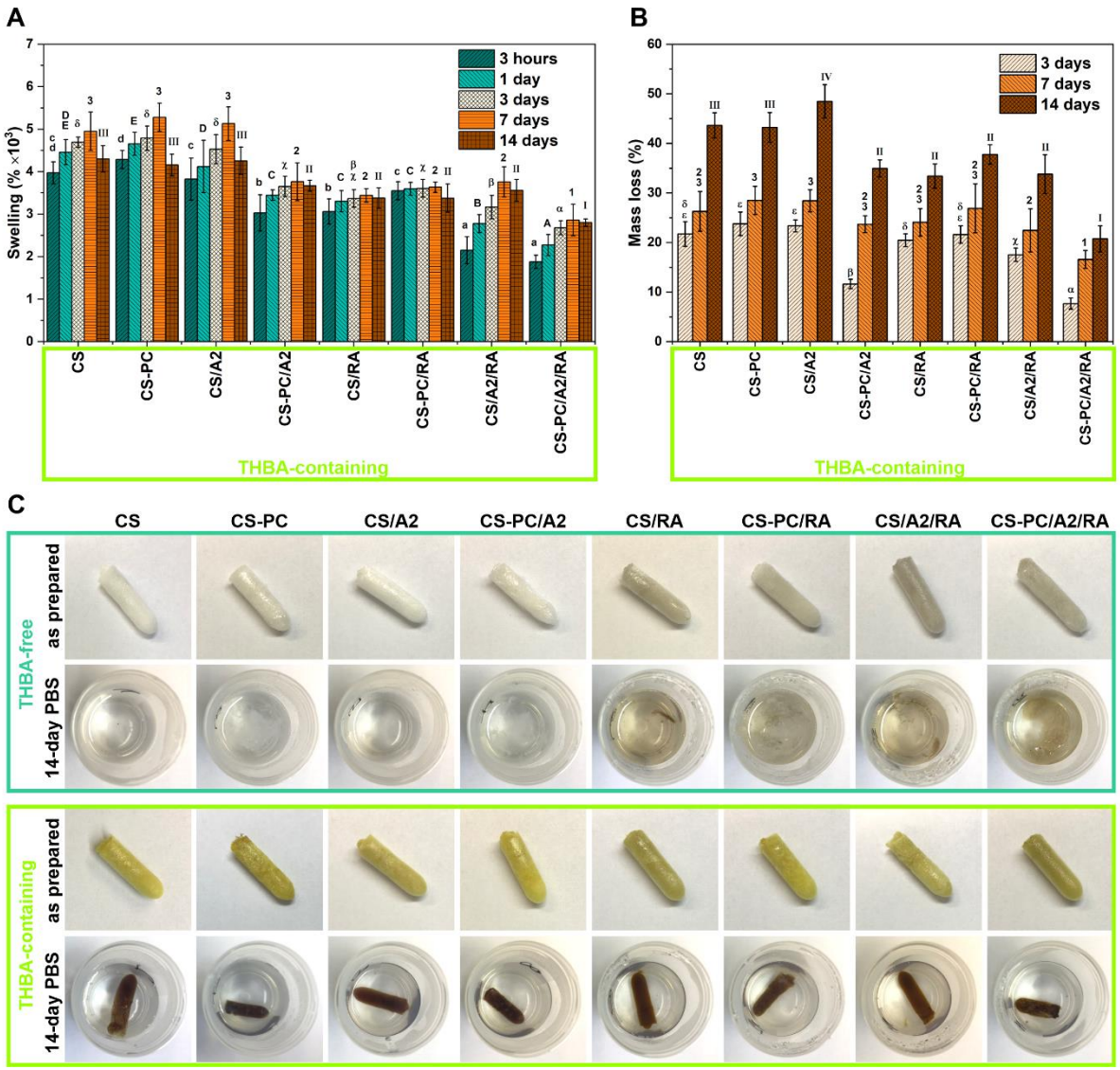

Figure 5. Swelling (A) and mass loss (B) of the THBA-containing hydrogels. Statistically significant differences ($p < 0.05$) between materials are indicated by subsequent lower (3 hours), upper (1 day) Latin letters, Greek letters (3 days), Arabic numerals (7 days), and Roman numerals (14 days). Different letters/numerals indicate statistically significant differences. Macroscopic images of the THBA-free and THBA-containing hydrogels before (as prepared) and after 14-day incubation in PBS (C).

Swelling and degradation behaviour of hydrogels crosslinked with THBA was investigated, because only these ones were able to maintain a sufficient integrity for accurate weighing (**Fig. 5C**). Materials swelled the most after the first 3 hours of incubation in PBS (1878-4287%). Swelling ability of all THBA-containing materials gradually increased with increasing incubation time until day 7 (**Fig. 5A**). After 14 days of incubation, a decrease in swelling was observed, which suggests that the dissolution process was accelerated. This is in agreement with the highest mass loss of hydrogels after 14-day incubation (**Fig. 5B**). Hydrogels containing RA and CS-PC/A2 material exhibited a lower decrease in swelling and lower mass loss after 14-day incubation compared to other materials. Furthermore, significantly lower water uptake and mass loss over the entire incubation period were observed for these materials. When comparing hydrogels with pectin, those ones modified with BG particles showed significantly reduced swelling and degradation. Importantly, materials combining all components (CS, PC, THBA, RA, BG) were the most stable.

Macroscopic observations showed that the materials crosslinked with THBA maintained shape and integrity over the entire incubation period. The THBA-free hydrogels containing pectin did not dissolve completely during 14-day incubation in PBS, in contrast to materials without this component (**Fig. 5C**). Also, hydrogels with RA exhibited incomplete dissolution in PBS, however debris were much smaller after 14-day incubation compared to materials with PC. THBA-free CS-PC/A2/RA hydrogel showed the lowest tendency to disintegrate/dissolve with a very high swelling rate.

Both swelling and degradation behaviour of hydrogels strongly depend on the degree of crosslinking and also the nature of linkage. In general, the higher the crosslinking degree, the lower the swelling ability and the slower the degradation rate (Hu et al., 2021; Iftime et al., 2017). Therefore, the results clearly indicated that THBA was successfully used as a crosslinking agent of CS-based hydrogels. The presence of PC, RA, and BG in THBA-free materials also induced crosslinking, but this effect was much weaker. This was due to the fact that the covalent bonding (Schiff base bond) is known to be much stronger than ionic

interactions (calcium-mediated interactions between PC chains and interactions between ionised functional groups of CS and PC) as well as hydrogen bonding (e.g. between hydroxyl groups of RA, BG, CS, and PC). The introduction of PC, RA, and BG into THBA-containing hydrogels gave a synergistic crosslinking effect.

Pornpimon and Sakamon (Pornpimon & Sakamon, 2010) showed that swelling of the chitosan films was reduced upon modification with the plant extract rich in polyphenols, as a result of intermolecular interactions between chitosan and the extract components. In contrast, literature data showed that the swelling ability and degradation rate of CS-based materials crosslinked with glutaraldehyde considerably increased upon addition of PC (Demir et al., 2020), while the presence of Ca^{2+} ions in CS-PC PEC materials accelerated the weight loss during incubation in PBS (Chen et al., 2010). It seems that THBA provided a stabilizing effect in CS-PC hydrogels, due to the hydrogen bonds established between the hydroxyl groups of THBA and pectin moieties. Furthermore, because of the lower content of pectin with respect to chitosan, PC-containing phase may be entrapped between highly crosslinked CS phases, creating a protective environment against water. This can be supported by µCT analysis (**Fig. 3**).

3.4. Antioxidant activity and release of biologically active compounds

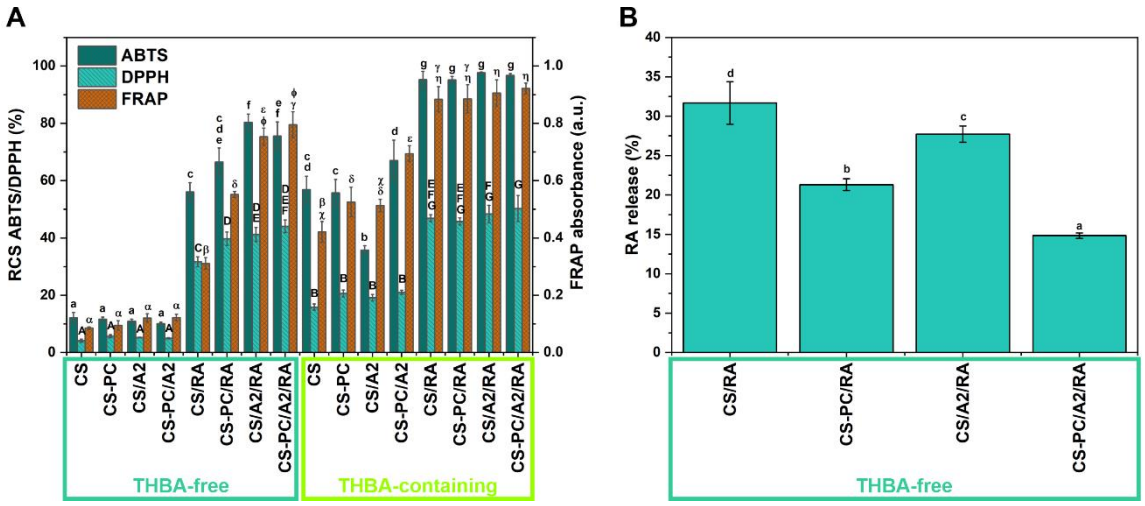

Figure 6. Radical scavenging capacity (RSC) against the $ABTS^{\bullet+}$ and $DPPH^{\bullet}$ radicals, as well as ferric reducing antioxidant potential (FRAP) of the THBA-free and THBA-containing hydrogels (A). Statistically significant differences ($p < 0.05$) are indicated by subsequent lower (ABTS), upper (DPPH) Latin letters and Greek letters (FRAP). The release of RA to PBS after 14-day incubation - % of the initial content in the materials (B). Statistically significant differences ($p < 0.05$) are indicated by subsequent lower Latin letters. Different letters indicate statistically significant differences.

The radical scavenging capacity (RSC) against the $ABTS^{\bullet+}$ and $DPPH^{\bullet}$ radicals, as well as the ferric reducing antioxidant potential (FRAP) of the hydrogels, are shown in **Fig. 6A**. Antioxidant activity of hydrogels can be clearly ascribed to the presence of phenolic components – THBA and RA. The materials containing these components showed high RSC and reducing potential which increased in the following order: THBA<RA<THBA+RA. In the case of materials with both THBA and RA, antioxidant potential did not depend on composition, in contrast to hydrogels with a single phenolic component (THBA or RA).

The release of biologically active compounds form hydrogels was evaluated after 14-day incubation in PBS (**Fig. 6B**). The release of THBA and RA form hydrogels crosslinked with THBA was below 1% of the initial content in the materials (data not shown). In the case of THBA-free hydrogels, release of RA was in the range 21% – 32%, depending on material composition. The presence of PC and BG separately decreased RA release significantly, while combination of these components (PC and BG) reduced RA release to the greatest extent. The release of RA from THBA-free hydrogels corresponded to yellowish colour of incubation medium (**Fig. 5C**).

A very low release level of THBA from THBA-containing hydrogels indicated its strong interactions with other components of the materials, confirming contribution in crosslinking process. Crosslinking with THBA inhibited almost completely the release of RA. In the case of THBA-free materials, RA release level corresponded with swelling/dissolution rate of the hydrogels (evaluated macroscopically – **Fig. 5C**). This indicates that, besides the interaction of RA with hydrogel components, the crosslinking process using THBA enables RA to be effectively entrapped in the hydrogel network. This is in agreement with other studies indicating that reduced release of biologically active components from the hydrogel is closely correlated with a higher degree of crosslinking and therefore lower swelling and degradation rates (Iftime et al., 2020; Karakurt et al., 2021).

Although THBA and RA were practically not released from the hydrogels crosslinked with THBA, they showed high antioxidant activity. Furthermore, the release level of RA from THBA-free hydrogels did not correlate with RSC and reducing potential. This may indicate that antioxidant activity of hydrogels is mainly attributed to antioxidants attached to the materials, not to the released ones (Dziadek, Dziadek, et al., 2021). Some differences in antioxidant activity between hydrogels containing a single phenolic compound (THBA or RA) may result from different interactions between them and other components (CS, PC, BG). As the antioxidant activity of a phenolic compound depends on the total number of phenolic hydroxyl

groups able to interact with reactive oxygen species by donating hydrogens, phenolic hydroxyl groups involved in hydrogen bonding were not available to scavenge free radicals/reduce ferric ions. In turn, the combination of both THBA and RA provided maximal antioxidant effect.

3.5. *In vitro* mineralisation studies

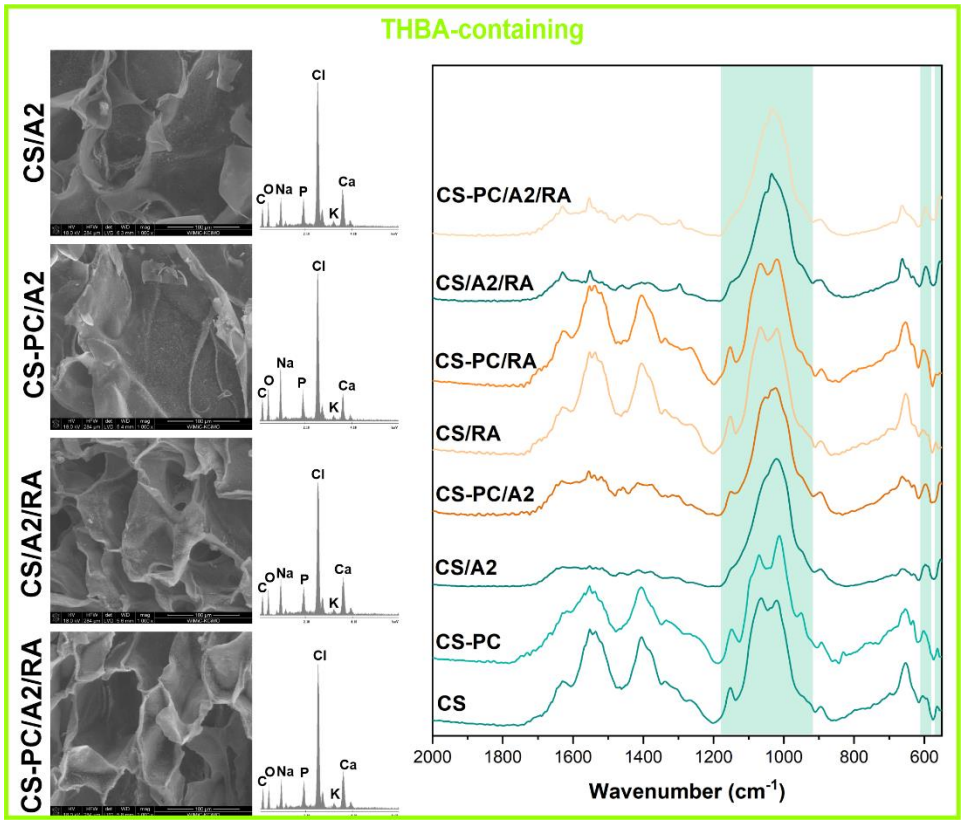

Figure 7. SEM images, EDX spectra, and ATR-FTIR spectra of the THBA-containing hydrogels after 14-day incubation in SBF.

Mineralisation process of the THBA-containing hydrogels after incubation in SBF was assessed using SEM/EDX and ATR-FTIR methods (**Fig. 7**). After 14-day incubation, hydrogels containing BG particles were covered with a uniform layer rich in calcium (Ca) and phosphorus (P). Furthermore, quite large amounts of sodium (Na), chlorine (Cl), and potassium (K) were incorporated into materials from SBF. In the case of crosslinked hydrogels without BG, only the latter elements (Na, Cl, K) were detected after incubation (data not shown). ATR-FTIR spectra of hydrogels containing BG particles incubated in SBF releveled new bands proving mineralisation by a CaP phase. Furthermore, the reduction in the intensity of bands arising from hydrogels was observed, indicating that the layer was thick and uniformly covered the materials. The bands noted in the ranges of 960 - 1130 cm^{-1} and 600 - 560 cm^{-1} correspond to

stretching and bending vibrations of PO_4^{3-} groups in crystalline CaP, respectively (Bossard et al., 2019). The bands in spectra of hydrogels containing RA tended to be sharper, compared to those without RA, suggesting the presence of CaP phase with higher crystallinity. This may be due to acceleration of CaP layer crystallization by additional polyphenolic compound with numerous phenolic hydroxyl groups capable to interact with Ca^{2+} ions from SBF (Zhou et al., 2012). There were no significant changes in the spectra of THBA-containing hydrogels without BG after incubation, confirming SEM/EDX analysis.

These results confirmed the mineralisation ability of CS- and CS-PC-based hydrogels containing BG particles. This may provide chemical bonding with bone, as well as improved mechanical properties of the hydrogels after implantation, actively promoting bone regeneration (Mota et al., 2012).

3.6. *In vitro* cell studies

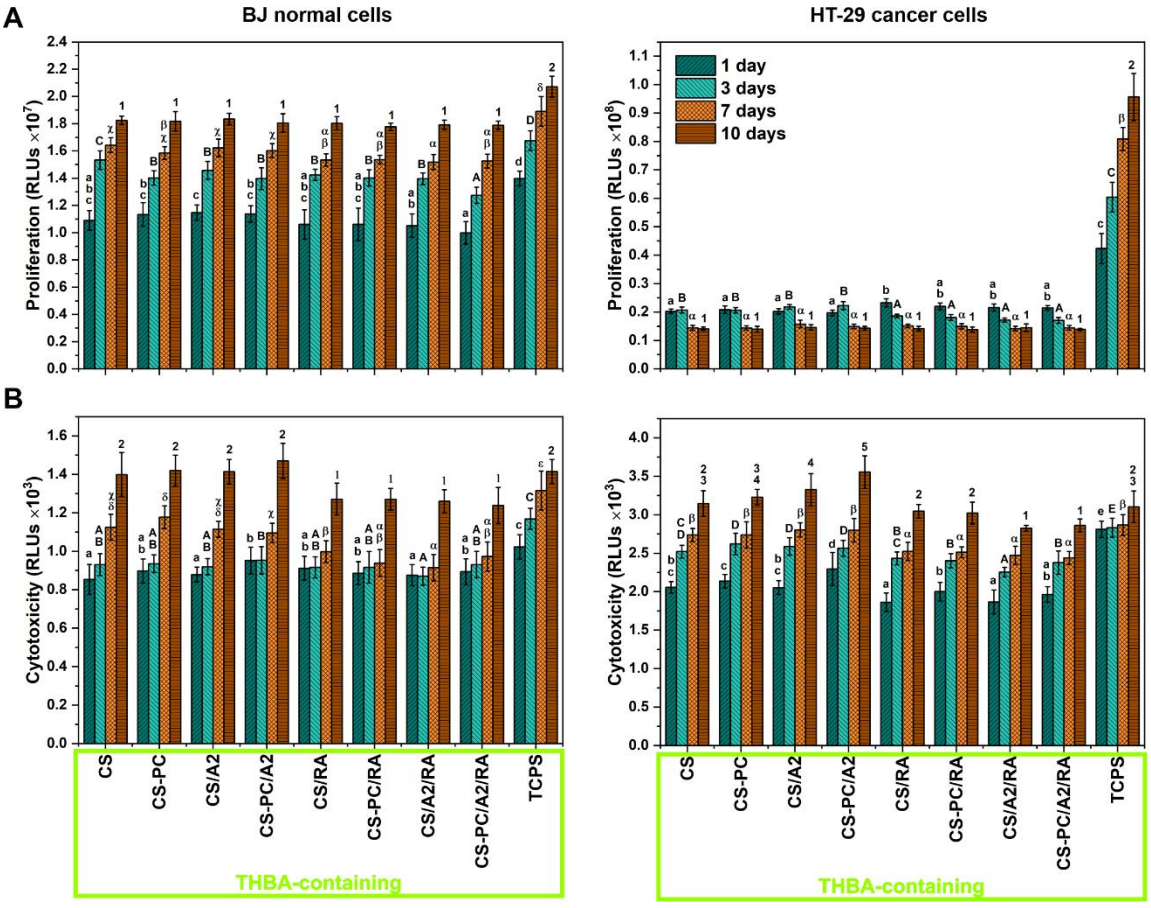

Figure 8. The response of BJ human normal skin fibroblasts and HT-29 human colon cancer epithelial cells cultured in contact with THBA-containing hydrogels: adenylate kinase (AK) level in the lysate corresponding to the number of intact adherent cells (A), AK level in the

supernatant representing material cytotoxicity (B). Statistically significant differences ($p < 0.05$) between materials and TCPS are indicated by subsequent lower (1 day), upper (3 days) Latin letters, Greek letters (7 days), Arabic numerals (10 days). Different letters indicate statistically significant differences.

Cytotoxicity and antiproliferative activity of THBA-containing hydrogels were evaluated on normal fibroblast cells and colon cancer cells (**Fig. 8**). The number of normal cells in contact with tested materials was lower after each cell culture period compared to the control (TCPS). Nevertheless, the fibroblasts cultured on hydrogels showed a high proliferation rate. After 10 days of culture, there were no statistically significant difference between materials. In the case of cancer cells, a strong antiproliferative activity of the materials was noted. The number of cancer cells in contact with the hydrogels was several times lower compared to TCPS and decreased with increasing culture time. In the case of materials containing RA, a significantly lower number of cells was observed after 3 days of culture, compared to hydrogels without RA. In turn, after 10-day culture, the number of cells in contact with materials did not differ significantly. Release of adenylate kinase from both normal and cancer cells in contact with hydrogels was on the same level or even lower compared to the control, indicating a low cytotoxic effect. Materials containing RA showed lower cytotoxicity when compared to unmodified ones.

The results showed that materials crosslinked with THBA were not cytotoxic against normal and cancer cells, however they inhibited the proliferation of cancer cells, possibly indicating a modulation of the cell cycle. This suggested that apoptosis rather than necrosis was a pathway for cancer cell death. Inducing apoptosis of cancer cells while reducing the death of normal cells is one of the most desirable mechanisms of action of anticancer therapies (Kwan et al., 2015). Antiproliferative activity of THBA-containing hydrogels may be ascribed to the presence of phenolic compounds – THBA and RA. As mentioned above, monoaldehydes, such as vanillin (Karakurt et al., 2021), salicylaldehyde (Iftime et al., 2017), o-vanillin, and 2,4,6-trihydroxybenzaldehyde (Marton et al., 2016), as well as polyphenols, for instance RA (Swamy et al., 2018), exhibited antitumor activity against different types of cancer cells. Similarly to antioxidant properties, anticancer activity was possibly attributed mainly to compounds attached to materials.

4. Conclusions

In the present work, a series of highly porous chitosan-based hydrogels was prepared and comprehensively evaluated. A simple and green method for crosslinking with the use of monoaldehyde - 2,3,4-trihydroxybenzaldehyde was successfully applied. The hydrogels were modified with a second hydrogel-forming polymer – pectin, as well as different functional additives – bioactive glass particles and rosmarinic acid. All of these were involved in the crosslinking process of the hydrogels, while simultaneously modulating their properties or imparting completely new ones. The crosslinking process with THBA resulted in significantly improved mechanical properties, high swelling capacity and delayed degradation. In addition to the crosslinking function, THBA provided high antioxidant activity and also a selective antiproliferative effect on cancer cells with no cytotoxicity for normal cells. Hydrogels containing pectin showed significantly modified microstructure and enhanced mechanical strength, while the combination with bioactive glass particles gave improved stability in PBS. All hydrogels modified with bioactive glass particles exhibited the ability to mineralize in SBF. The addition of rosmarinic acid enhanced antioxidant and anticancer activities as well as promoting the mineralisation process. The results indicated that the obtained hydrogels represent promising multifunctional biomaterials with a wide range of tunable physicochemical and biological properties with great potential for the use in different tissue engineering fields, for instance in bone regeneration or after tumour resection.

5. Acknowledgments

This work was supported by the National Science Centre, Poland, grant nos. 2017/27/B/ST8/00195 (KCK) and 2019/32/C/ST5/00386 (MD). The μCT investigations were possible due to European Regional Development Fund through Competitiveness Operational Program 2014-2020, Priority axis 1, ID P_36_611, MySMIS code 107066, INOVABIOMED (AS, ICS). This work was partly supported by program „Excellence initiative – research university" for the AGH University of Science and Technology. The authors thank Herbstreith & Fox Company (Germany) for delivering pectin.

6. Literature

Birch, N. P., Barney, L. E., Pandres, E., Peyton, S. R., & Schiffman, J. D. (2015). Thermal-Responsive Behavior of a Cell Compatible Chitosan/Pectin Hydrogel. *Biomacromolecules*, *16*(6), 1837–1843. https://doi.org/10.1021/ACS.BIOMAC.5B00425

Bossard, C., Granel, H., Jallot, É., Montouillout, V., Fayon, F., Soulié, J., Drouet, C., Wittrant, Y., & Lao, J. (2019). Mechanism of Calcium Incorporation Inside Sol–Gel Silicate Bioactive Glass and the Advantage of Using Ca(OH)2 over Other Calcium

Sources. *ACS Biomaterials Science & Engineering*, *5*(11), 5906–5915. https://doi.org/10.1021/ACSBIOMATERIALS.9B01245

Chen, P. H., Kuo, T. Y., Kuo, J. Y., Tseng, Y. P., Wang, D. M., Lai, J. Y., & Hsieh, H. J. (2010). Novel chitosan–pectin composite membranes with enhanced strength, hydrophilicity and controllable disintegration. *Carbohydrate Polymers*, *82*(4), 1236–1242. https://doi.org/10.1016/J.CARBPOL.2010.06.057

Coimbra, P., Ferreira, P., de Sousa, H. C., Batista, P., Rodrigues, M. A., Correia, I. J., & Gil, M. H. (2011). Preparation and chemical and biological characterization of a pectin/chitosan polyelectrolyte complex scaffold for possible bone tissue engineering applications. *International Journal of Biological Macromolecules*, *48*(1), 112–118. https://doi.org/10.1016/J.IJBIOMAC.2010.10.006

Craciun, A. M., Mititelu Tartau, L., Pinteala, M., & Marin, L. (2019). Nitrosalicyl-imine-chitosan hydrogels based drug delivery systems for long term sustained release in local therapy. *Journal of Colloid and Interface Science*, *536*, 196–207. https://doi.org/10.1016/J.JCIS.2018.10.048

Cui, S., Yao, B., Gao, M., Sun, X., Gou, D., Hu, J., Zhou, Y., & Liu, Y. (2017). Effects of pectin structure and crosslinking method on the properties of crosslinked pectin nanofibers. *Carbohydrate Polymers*, *157*, 766–774. https://doi.org/10.1016/J.CARBPOL.2016.10.052

Demir, D., Ceylan, S., Göktürk, D., & Bölgen, N. (2020). Extraction of pectin from albedo of lemon peels for preparation of tissue engineering scaffolds. *Polymer Bulletin 2020 78:4*, *78*(4), 2211–2226. https://doi.org/10.1007/S00289-020-03208-1

Douglas, T. E. L., Dziadek, M., Schietse, J., Boone, M., Declercq, H. A., Coenye, T., Vanhoorne, V., Vervaet, C., Balcaen, L., Buchweitz, M., Vanhaecke, F., van Assche, F., Cholewa-Kowalska, K., & Skirtach, A. G. (2019). Pectin-bioactive glass self-gelling, injectable composites with high antibacterial activity. *Carbohydrate Polymers*, *205*, 427–436. https://doi.org/10.1016/J.CARBPOL.2018.10.061

Douglas, T. E. L., Kumari, S., Dziadek, K., Dziadek, M., Abalymov, A., Cools, P., Brackman, G., Coenye, T., Morent, R., Mohan, M. K., & Skirtach, A. G. (2017). Titanium surface functionalization with coatings of chitosan and polyphenol-rich plant extracts. *Materials Letters*, *196*, 213–216. https://doi.org/10.1016/J.MATLET.2017.03.065

Dziadek, M., Charuza, K., Kudlackova, R., Aveyard, J., D'Sa, R., Serafim, A., Stancu, I. C., Iovu, H., Kerns, J. G., Allinson, S., Dziadek, K., Szatkowski, P., Cholewa-Kowalska, K., Bacakova, L., Pamula, E., & Douglas, T. E. L. (2021). Modification of heat-induced whey protein isolate hydrogel with highly bioactive glass particles results in promising biomaterial for bone tissue engineering. *Materials & Design*, *205*, 109749. https://doi.org/10.1016/J.MATDES.2021.109749

Dziadek, M., Dziadek, K., Checinska, K., Zagrajczuk, B., Golda-Cepa, M., Brzychczy-Wloch, M., Menaszek, E., Kopec, A., & Cholewa-Kowalska, K. (2021). PCL and PCL/bioactive glass biomaterials as carriers for biologically active polyphenolic compounds: Comprehensive physicochemical and biological evaluation. *Bioactive Materials*, *6*(6), 1811–1826. https://doi.org/10.1016/J.BIOACTMAT.2020.11.025

Dziadek, M., Kudlackova, R., Zima, A., Slosarczyk, A., Ziabka, M., Jelen, P., Shkarina, S., Cecilia, A., Zuber, M., Baumbach, T., Surmeneva, M. A., Surmenev, R. A., Bacakova, L., Cholewa-Kowalska, K., & Douglas, T. E. L. (2019). Novel multicomponent organic–inorganic WPI/gelatin/CaP hydrogel composites for bone tissue engineering. *Journal of Biomedical Materials Research Part A*, *107*(11), 2479–2491. https://doi.org/10.1002/JBM.A.36754

Gao, C., Wang, S., Liu, B., Yao, S., Dai, Y., Zhou, L., Qin, C., & Fatehi, P. (2021). Sustainable Chitosan-Dialdehyde Cellulose Nanocrystal Film. *Materials 2021, Vol. 14, Page 5851*, *14*(19), 5851. https://doi.org/10.3390/MA14195851

Hu, J., Wang, Z., Miszuk, J. M., Zhu, M., Lansakara, T. I., Tivanski, A. v., Banas, J. A., & Sun, H. (2021). Vanillin-bioglass cross-linked 3D porous chitosan scaffolds with strong osteopromotive and antibacterial abilities for bone tissue engineering. *Carbohydrate Polymers*, *271*, 118440. https://doi.org/10.1016/J.CARBPOL.2021.118440

Iftime, M. M., Mititelu Tartau, L., & Marin, L. (2020). New formulations based on salicyl-imine-chitosan hydrogels for prolonged drug release. *International Journal of Biological Macromolecules*, *160*, 398–408. https://doi.org/10.1016/J.IJBIOMAC.2020.05.207

Iftime, M. M., Morariu, S., & Marin, L. (2017). Salicyl-imine-chitosan hydrogels: Supramolecular architecturing as a crosslinking method toward multifunctional hydrogels. *Carbohydrate Polymers*, *165*, 39–50. https://doi.org/10.1016/J.CARBPOL.2017.02.027

Iviglia, G., Cassinelli, C., Bollati, D., Baino, F., Torre, E., Morra, M., & Vitale-Brovarone, C. (2016). Engineered porous scaffolds for periprosthetic infection prevention. *Materials Science and Engineering: C*, *68*, 701–715. https://doi.org/10.1016/J.MSEC.2016.06.050

Karakurt, I., Ozaltin, K., Vargun, E., Kucerova, L., Suly, P., Harea, E., Minařík, A., Štěpánková, K., Lehocky, M., Humpolícek, P., Vesel, A., & Mozetic, M. (2021). Controlled release of enrofloxacin by vanillin-crosslinked chitosan-polyvinyl alcohol blends. *Materials Science and Engineering: C*, *126*, 112125. https://doi.org/10.1016/J.MSEC.2021.112125

Kokubo, T., & Takadama, H. (2006). How useful is SBF in predicting in vivo bone bioactivity? *Biomaterials*, *27*(15), 2907–2915. https://doi.org/10.1016/J.BIOMATERIALS.2006.01.017

Kuhlmann, A., & Röhl, C. (2008). Phenolic Antioxidant Compounds Produced by in Vitro. Cultures of Rosemary (Rosmarinus officinalis.) and Their Anti-inflammatory Effect on Lipopolysaccharide-Activated Microglia. *Http://Dx.Doi.Org/10.1080/13880200600794063*, *44*(6), 401–410. https://doi.org/10.1080/13880200600794063

Kwan, Y. P., Saito, T., Ibrahim, D., Al-Hassan, F. M. S., Oon, C. E., Chen, Y., Jothy, S. L., Kanwar, J. R., & Sasidharan, S. (2015). Evaluation of the cytotoxicity, cell-cycle arrest, and apoptotic induction by Euphorbia hirta in MCF-7 breast cancer cells. *Https://Doi.Org/10.3109/13880209.2015.1064451*, *54*(7), 1223–1236. https://doi.org/10.3109/13880209.2015.1064451

Lee, J.-W., Asai, M., Jeon, S.-K., Iimura, T., Yonezawa, T., Cha, B.-Y., Woo, J.-T., & Yamaguchi, A. (2015). Rosmarinic acid exerts an antiosteoporotic effect in the RANKL-induced mouse model of bone loss by promotion of osteoblastic differentiation and inhibition of osteoclastic differentiation. *Molecular Nutrition & Food Research*, *59*(3), 386–400. https://doi.org/10.1002/MNFR.201400164

Li, J., Zhu, D., Yin, J., Liu, Y., Yao, F., & Yao, K. (2010). Formation of nano-hydroxyapatite crystal in situ in chitosan–pectin polyelectrolyte complex network. *Materials Science and Engineering: C*, *30*(6), 795–803. https://doi.org/10.1016/J.MSEC.2010.03.011

Luppi, B., Bigucci, F., Abruzzo, A., Corace, G., Cerchiara, T., & Zecchi, V. (2010). Freeze-dried chitosan/pectin nasal inserts for antipsychotic drug delivery. *European Journal of Pharmaceutics and Biopharmaceutics*, *75*(3), 381–387. https://doi.org/10.1016/J.EJPB.2010.04.013

Maciel, V. B. v., Yoshida, C. M. P., & Franco, T. T. (2015). Chitosan/pectin polyelectrolyte complex as a pH indicator. *Carbohydrate Polymers*, *132*, 537–545. https://doi.org/10.1016/J.CARBPOL.2015.06.047

Mallick, S. P., Suman, D. K., Singh, B. N., Srivastava, P., Siddiqui, N., Yella, V. R., Madhual, A., & Vemuri, P. K. (2020). Strategies toward development of biodegradable hydrogels for biomedical applications. *Https://Doi.Org/10.1080/25740881.2020.1719135*, *59*(9), 911–927. https://doi.org/10.1080/25740881.2020.1719135

Marin, L., Moraru, S., Popescu, M. C., Nicolescu, A., Zgardan, C., Simionescu, B. C., & Barboiu, M. (2014). Out-of-Water Constitutional Self-Organization of Chitosan–Cinnamaldehyde Dynagels. *Chemistry – A European Journal*, *20*(16), 4814–4821. https://doi.org/10.1002/CHEM.201304714

Martínez, A., Blanco, M. D., Davidenko, N., & Cameron, R. E. (2015). Tailoring chitosan/collagen scaffolds for tissue engineering: Effect of composition and different crosslinking agents on scaffold properties. *Carbohydrate Polymers*, *132*, 606–619. https://doi.org/10.1016/J.CARBPOL.2015.06.084

Martins, J. G., de Oliveira, A. C., Garcia, P. S., Kipper, M. J., & Martins, A. F. (2018). Durable pectin/chitosan membranes with self-assembling, water resistance and enhanced mechanical properties. *Carbohydrate Polymers*, *188*, 136–142. https://doi.org/10.1016/J.CARBPOL.2018.01.112

Marton, A., Kúsz, E., Kolozsi, C., Tubak, V., Zagotto, G., Buzás, K., Quintieri, L., & Vizler, C. (2016). Vanillin analogues o-vanillin and 2,4,6-trihydroxybenzaldehyde inhibit NFκB activation and suppress growth of A375 human melanoma. *Anticancer Research*, *36*(11), 5743–5750. https://doi.org/10.21873/anticanres.11157

Montaser, A. S., Wassel, A. R., & Al-Shaye'a, O. N. (2019). Synthesis, characterization and antimicrobial activity of Schiff bases from chitosan and salicylaldehyde/TiO2 nanocomposite membrane. *International Journal of Biological Macromolecules*, *124*, 802–809. https://doi.org/10.1016/J.IJBIOMAC.2018.11.229

Mota, J., Yu, N., Caridade, S. G., Luz, G. M., Gomes, M. E., Reis, R. L., Jansen, J. A., Frank Walboomers, X., & Mano, J. F. (2012). Chitosan/bioactive glass nanoparticle composite membranes for periodontal regeneration. *Acta Biomaterialia*, *8*(11), 4173–4180. https://doi.org/10.1016/J.ACTBIO.2012.06.040

Munarin, F., Guerreiro, S. G., Grellier, M. A., Tanzi, M. C., Barbosa, M. A., Petrini, P., & Granja, P. L. (2011). Pectin-Based Injectable Biomaterials for Bone Tissue Engineering. *Biomacromolecules*, *12*(3), 568–577. https://doi.org/10.1021/BM101110X

Neufeld, L., & Bianco-Peled, H. (2017). Pectin–chitosan physical hydrogels as potential drug delivery vehicles. *International Journal of Biological Macromolecules*, *101*, 852–861. https://doi.org/10.1016/J.IJBIOMAC.2017.03.167

Neves, S. C., Gomes, D. B., Sousa, A., Bidarra, S. J., Petrini, P., Moroni, L., Barrias, C. C., & Granja, P. L. (2015). Biofunctionalized pectin hydrogels as 3D cellular microenvironments. *Journal of Materials Chemistry B*, *3*(10), 2096–2108. https://doi.org/10.1039/C4TB00885E

Olaru, A. M., Marin, L., Morariu, S., Pricope, G., Pinteala, M., & Tartau-Mititelu, L. (2018). Biocompatible chitosan based hydrogels for potential application in local tumour therapy. *Carbohydrate Polymers*, *179*, 59–70. https://doi.org/10.1016/J.CARBPOL.2017.09.066

Pornpimon, M., & Sakamon, D. (2010). Effects of drying methods and conditions on release characteristics of edible chitosan films enriched with Indian gooseberry extract. *Food Chemistry*, *118*(3), 594–601. https://doi.org/10.1016/J.FOODCHEM.2009.05.027

Sitarz, M., Bulat, K., Wajda, A., & Szumera, M. (2013). Direct crystallization of silicate-phosphate glasses of NaCaPO 4-SiO2 system. *Journal of Thermal Analysis and Calorimetry*, *113*(3), 1363–1368. https://doi.org/10.1007/S10973-013-3240-Y/FIGURES/7

Stroescu, M., Stoica-Guzun, A., Isopencu, G., Jinga, S. I., Parvulescu, O., Dobre, T., & Vasilescu, M. (2015). Chitosan-vanillin composites with antimicrobial properties. *Food Hydrocolloids*, *48*, 62–71. https://doi.org/10.1016/J.FOODHYD.2015.02.008

Swamy, M. K., Sinniah, U. R., & Ghasemzadeh, A. (2018). Anticancer potential of rosmarinic acid and its improved production through biotechnological interventions and functional genomics. *Applied Microbiology and Biotechnology 2018 102:18*, *102*(18), 7775–7793. https://doi.org/10.1007/S00253-018-9223-Y

Wajda, A., Bułat, K., & Sitarz, M. (2016). Structure and microstructure of the glasses from NaCaPO4–SiO2 and NaCaPO4–SiO2–AlPO4 systems. *Journal of Molecular Structure*, *1126*, 47–62. https://doi.org/10.1016/J.MOLSTRUC.2015.12.003

Wajda, A., Goldmann, W. H., Detsch, R., Grünewald, A., Boccaccini, A. R., & Sitarz, M. (2018). Structural characterization and evaluation of antibacterial and angiogenic potential of gallium-containing melt-derived and gel-derived glasses from CaO-SiO2 system. *Ceramics International*, *44*(18), 22698–22709. https://doi.org/10.1016/J.CERAMINT.2018.09.051

Xavier, C. P. R., Lima, C. F., Fernandes-Ferreira, M., & Pereira-Wilson, C. (2009). Salvia Fruticosa, Salvia Officinalis, and Rosmarinic Acid Induce Apoptosis and Inhibit Proliferation of Human Colorectal Cell Lines: The Role in MAPK/ERK Pathway. *Http://Dx.Doi.Org/10.1080/01635580802710733*, *61*(4), 564–571. https://doi.org/10.1080/01635580802710733

Xu, C., Zhan, W., Tang, X., Mo, F., Fu, L., & Lin, B. (2018). Self-healing chitosan/vanillin hydrogels based on Schiff-base bond/hydrogen bond hybrid linkages. *Polymer Testing*, *66*, 155–163. https://doi.org/10.1016/J.POLYMERTESTING.2018.01.016

Yuliarti, O., Hoon, A. L. S., & Chong, S. Y. (2017). Influence of pH, pectin and Ca concentration on gelation properties of low-methoxyl pectin extracted from Cyclea barbata Miers. *Food Structure*, *11*, 16–23. https://doi.org/10.1016/J.FOOSTR.2016.10.005

Zagrajczuk, B., Dziadek, M., Olejniczak, Z., Cholewa-Kowalska, K., & Laczka, M. (2017). Structural and chemical investigation of the gel-derived bioactive materials from the SiO2–CaO and SiO2-CaO-P2O5 systems. *Ceramics International*, *43*(15), 12742–12754. https://doi.org/10.1016/J.CERAMINT.2017.06.160

Zhang, M., Yang, M., Woo, M. W., Li, Y., Han, W., & Dang, X. (2021). High-mechanical strength carboxymethyl chitosan-based hydrogel film for antibacterial wound dressing. *Carbohydrate Polymers*, *256*, 117590. https://doi.org/10.1016/J.CARBPOL.2020.117590

Zhang, Y., Shi, X., Yu, Y., Zhao, S., Song, H., Chen, A., & Shang, Z. (2014). Preparation and Characterization of Vanillin Cross-Linked Chitosan Microspheres of Pterostilbene. *Http://Dx.Doi.Org/10.1080/1023666X.2014.864488*, *19*(1), 83–93. https://doi.org/10.1080/1023666X.2014.864488

Zhou, R., Si, S., & Zhang, Q. (2012). Water-dispersible hydroxyapatite nanoparticles synthesized in aqueous solution containing grape seed extract. *Applied Surface Science*, *258*(8), 3578–3583. https://doi.org/10.1016/J.APSUSC.2011.11.119

Newly crosslinked chitosan- and chitosan-pectin-based hydrogels with high antioxidant and potential anticancer activity

Michal Dziadek [a,b*], Kinga Dziadek [c], Szymon Salagierski [b], Mariola Drozdowska [c], Andrada Serafim [d], Izabela-Cristina Stancu [d], Piotr Szatkowski [e], Aneta Kopec [c], Izabella Rajzer [f], Timothy E. L. Douglas [g,h], Katarzyna Cholewa-Kowalska [b]

[a] Faculty of Chemistry, Jagiellonian University, Krakow, Poland;
[b] Department of Glass Technology and Amorphous Coatings, AGH University of Science and Technology, Krakow, Poland;
[c] Department of Human Nutrition and Dietetics, University of Agriculture in Krakow, Krakow, Poland;
[d] Advanced Polymer Materials Group, University Politehnica of Bucharest, Bucharest, Romania;
[e] Department of Biomaterials and Composites, AGH University of Science and Technology, Krakow, Poland;
[f] Department of Mechanical Engineering Fundamentals, ATH University of Bielsko-Biala, Bielsko-Biała, Poland;
[g] Engineering Department, Lancaster University, Lancaster, United Kingdom;
[h] Materials Science Institute (MSI), Lancaster University, Lancaster, United Kingdom;

*corresponding author: michal.dziadek@uj.edu.pl, dziadek@agh.edu.pl

Abstract

Monoaldehydes, due to natural origin and therapeutic activity, have attracted great attention for their ability to crosslink chitosan hydrogels for biomedical applications. However, most studies have focused on single-component hydrogels. In this work, chitosan-based hydrogels, crosslinked for the first time with 2,3,4-trihydroxybenzaldehyde (THBA), were modified with pectin (PC), bioactive glass (BG), and rosmarinic acid (RA). All of these were not only involved in the crosslinking, but also modulated properties or imparted completely new ones. THBA functioned as a crosslinker, resulting in improved mechanical properties, high swelling capacity and delayed degradation and also imparted high antioxidant activity and antiproliferative effect on cancer cells without cytotoxicity for normal cells. Hydrogels containing PC showed enhanced mechanical strength, while the combination with BG gave improved stability in PBS. All hydrogels modified with BG exhibited the ability to mineralize in SBF. The addition of RA enhanced antioxidant and anticancer activities and promoting the mineralisation process.

Keywords: monoaldehyde; polyelectrolyte complex; bioactive glass; polyphenols; micro-computed tomography

1. Introduction

Hydrogel materials are able to absorb a large amounts of water and swell without dissolving in aqueous media. These unique properties hydrogels owe to three-dimensional crosslinked network of hydrophilic polymer chains. Recently, hydrogels have attracted great attention for their potential application in a wide range of biomedical areas, including tissue engineering and controlled drug delivery systems. This is due to the fact that hydrogels are able to mimic biomechanical characteristics of native extracellular matrix (ECM), providing 3D microenvironments for cell migration, adhesion, and proliferation, as well as promoting the transport of nutrients and signalling molecules. Furthermore, their porosity, high swelling ability, and hydrophilic nature make hydrogels excellent candidates as carriers of hydrophilic biologically active compounds (e.g. drugs, biomolecules, phytochemicals). Generally, all of these properties of hydrogels are highly associated with the degree of crosslinking (Mallick et al., 2020; M. Zhang et al., 2021).

Chitosan (CS), as a glucosamine-based polysaccharide obtained by deacetylation of chitin, is one of the most studied biopolymers in the biomedical applications. CS is characterised by good biocompatibility, biodegradability, inherent antibacterial activity, hemostatic potential, wide availability, and low price (Coimbra et al., 2011). Although CS-based hydrogels for biomedical

applications have been widely studied in recent years, their effective and safe crosslinking still remains a great challenge.

The most frequently used crosslinking agents of CS are dialdehydes, in particular glutaraldehyde (GA). The crosslinking mechanism of dialdehydes, including GA, is based on the formation of imine bonds, well-known as Schiff bases, between two aldehyde groups of GA and amino groups of chitosan chains. However, GA is highly cytotoxic and neurotoxic. In recent years, great interest has been focused on monoaldehydes as CS crosslinking agent, which in many cases, unlike dialdehydes, are naturally occurring compounds with beneficial biological activities (e.g. antioxidant, anticancer, antibacterial) (Iftime et al., 2017; Xu et al., 2018). The crosslinking mechanism of the monoaldehyde is based on imine-bond formation between the single aldehyde group of the monoaldehyde molecule and the amino group of the CS chain accompanied by the hydrophilic/hydrophobic assembling of the CS/aromatic units of the monoaldehyde. The monoaldehyde hydroxyl group in the *ortho* position can form an intramolecular hydrogen bond with the imine nitrogen, providing the stabilization of the imine linkage (Iftime et al., 2017). Furthermore, the hydroxyl groups in other positions can form additional hydrogen bonds with the hydroxyl or the amino groups in chitosan chains, enhancing the crosslinking effect (Xu et al., 2018).

The second important crosslinking mechanism of CS is ionic/electrostatic interaction. Examples of this are polyelectrolyte complexes (PECs), which are formed by electrostatic interactions between cationic amino groups in CS and anionic groups in other polymers, such as carboxyl acid groups of pectin (PC) under specific pH conditions (in the p*K*a range of these two polymers) (Maciel et al., 2015).

PCs are anionic polysaccharides derived mainly from by-products of the fruit processing industry, therefore they are environmentally friendly, available in vast amounts and inexpensive (Neves et al., 2015). PCs show good biocompatibility and biodegradability, as well as a wide range of biological activities, such as anti-inflammatory, antioxidant, and anticancer properties (Cui et al., 2017; Munarin et al., 2011; Neves et al., 2015). PCs, especially low esterified amidated ones, can easily be crosslinked by calcium ions to form hydrogels, also injectable systems (Yuliarti et al., 2017). For these reasons, PCs are receiving increased attention as a hydrogel material for drug delivery and tissue engineering applications (Cui et al., 2017; Douglas et al., 2019; Munarin et al., 2011; Neves et al., 2015).

A combination of CS and PC to obtain PEC hydrogels exploits the biological benefits of both biopolymers while also enabling modification of the material properties, such as mechanical behaviour, wettability, swelling, and degradation (Chen et al., 2010; Coimbra et al., 2011).

CS/PC-based hydrogels showed high cytocompatibility with many cell types (Birch et al., 2015; Li et al., 2010), capacity to be loaded with drugs (Luppi et al., 2010; Neufeld & Bianco-Peled, 2017) and natural biological active compounds (Maciel et al., 2015), indicating high potential in biomedical applications.

In order to improve the biological and physicochemical properties of hydrogels or impart completely new functionalities to them, various additives are used. One of them is bioactive ceramic, especially bioactive glass (BG). BGs have significantly altered the properties of hydrogels relevant for bone regeneration applications (mechanical properties, microstructural/topographical features, osteoblast activity) (Dziadek, Charuza, et al., 2021). Furthermore, calcium phosphate (CaP) forming ability of BGs and osteogenic properties of their dissolution products (i.a. silica, calcium ions) have induced hydrogel mineralization with a CaP phase, assuring improved mechanical properties, direct chemical bonding with bone, and stimulation of bone regeneration (Sitarz et al., 2013; Wajda et al., 2016, 2018). Other additives used in hydrogels are biologically active compounds. In recent years, much attention has been paid to naturally occurring chemicals - polyphenols, as alternative for drugs and biomolecules. This is due to the multiple biological activities of polyphenols, such as antioxidant, anticancer, anti-inflammatory, antimicrobial and osteostimulation properties, and minor side effects (Dziadek, Dziadek, et al., 2021). One of the polyphenols frequently found in herbal plants is rosmarinic acid (RA). RA has exhibited multi-faceted activity, for instance strong antioxidant, anticancer, and anti-inflammatory activities (Kuhlmann & Röhl, 2008; Xavier et al., 2009). Furthermore, RA has been shown to regulate bone metabolism by inducing osteoblast differentiation and inhibiting osteoclast activity (Lee et al., 2015).

As we have shown in previous work, calcium-rich sol-gel-derived BG particles can be a sufficient rich source of Ca^{2+} ions for internal crosslinking of low esterified amidated PC (Douglas et al., 2019). Furthermore, numerous silanol groups (Si-OH) of sol-gel-derived BG and hydroxyl groups of polyphenolic compounds may interact with each other and also with functional moieties of chitosan (-OH, $-NH_2$) and pectin (-OH, -COOH) to form hydrogen bonds (Douglas et al., 2017; Dziadek, Dziadek, et al., 2021; Hu et al., 2021).

In this work, the phenolic monoaldehyde - 2,3,4-trihydroxybenzaldehyde (THBA) was used for the first time as a crosslinking agent in CS-based hydrogels for potential use in tissue engineering applications. It was hypothesize that the use of a second hydrogel-forming polymer, namely PC, as well as different functional additives, including calcium-rich sol-gel-derived BG particles and polyphenolic compounds (RA) would significantly affect the crosslinking process, and therefore the properties of CS-based hydrogels. A series of highly porous scaffolds was

evaluated in terms of (i) microstructure and porosity; (ii) mechanical properties; (iii) thermal properties; (iv) swelling and degradation behaviour; (v) the *in vitro* mineralisation process; (vi) antioxidant activity; (vii) *in vitro* cytotoxicity and antiproliferative activity against normal and cancer human cells.

2. Materials and methods

2.1. Preparation of the materials

Bioactive glass powder of the following composition (%mol) 54CaO-40SiO_2-6P_2O_5, denoted as A2, was synthetized using a sol-gel technique as reported previously (Zagrajczuk et al., 2017). BG was milled in an attritor with ZrO_2 balls in isopropyl alcohol medium to obtain a powder with a particle size of 1 μm (d_{50}). The particle size distribution and SEM image of BG are shown in **Fig. A.1**. Particle size distribution was measured by laser diffraction Mastersizer-S equipment (Malvern Instruments, UK) as described previously (Douglas et al., 2019).

Hydrogels were prepared using freeze-drying process. Chitosan (medium molecular weight; 75-85% deacetylated; Sigma-Aldrich, Germany) and pectin (low esterified amidated pectin from citrus peels; degree of esterification - 27.4%, degree of amidation - 22.8%, galacturonic acid content - 93.5%; Herbstreith & Fox, Germany) solutions (2 w/v%) were prepared by dissolving CS and PC powders in 1 v/v% acetic acid aqueous solution and deionised water, respectively. The pH values of the polymer solutions were 4.5 and 4.4, respectively. 2,3,4-trihydroxybenzaldehyde (Sigma-Aldrich, Germany) was used as crosslinking agent. Materials with and without THBA were prepared. THBA, rosmarinic acid (Carbosynth Ltd, UK), and BG powder was introduced into materials in the form of 1 w/v% solution/suspension in deionised water. Adequate solutions/suspensions (CS/PC/THBA/RA/BG) were mixed (3000 rpm) at room temperature in 2-mL Eppendorf tubes using a vortexer to obtain materials of compositions presented in **Table 1**. All mixtures were filled up to constant volume using 1 v/v% acetic acid. The scheme showing the order of mixing of the components is shown in **Fig. 1A** (if a particular component was not added, the respective mixing step for that component was omitted). The samples in Eppendorf tubes were frozen in a laboratory freezer at -24 ℃ for 48 h and then freeze-dried (Alpha 1–4 LSCplus, Christ, Germany, ice condenser temperature -55 °C, vacuum 0.1 mbar) for 48 h.

Table 1. The compositions of materials.

Material	CS (w/w%)	PC (w/w%)	THBA (w/w%)	RA (w/w%)	A2 BG (w/w%)
Uncrosslinked materials					
CS	100	-	-	-	-
CS-PC	70	30	-	-	-
CS/A2	100	-	-	-	5
CS-PC/A2	70	30	-	-	5
CS/RA	100	-	-	2	-
CS-PC/RA	70	30	-	2	-
CS/A2/RA	100	-	-	2	5
CS-PC/A2/RA	70	30	-	2	5
Crosslinked materials					
CS	100	-	2	-	-
CS-PC	70	30	2	-	-
CS/A2	100	-	2	-	5
CS-PC/A2	70	30	2	-	5
CS/RA	100	-	2	2	-
CS-PC/RA	70	30	2	2	-
CS/A2/RA	100	-	2	2	5
CS-PC/A2/RA	70	30	2	2	5

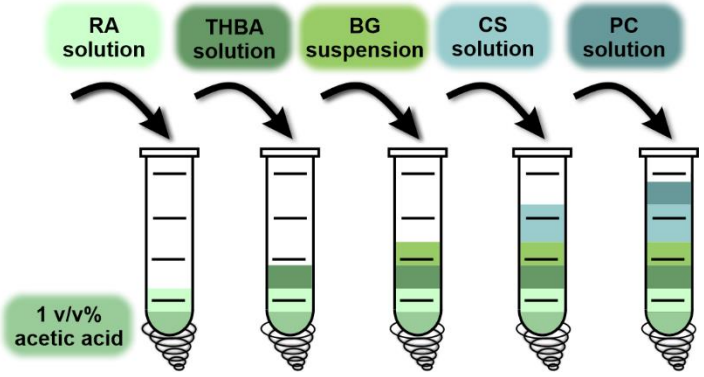

Figure 1. Scheme showing the order of mixing of the components (if a particular component was not added, the mixing step for that component was omitted).

2.2. Microstructure analysis

THBA-free and THBA-containing hydrogels were analysed using ultra-high resolution scanning electron microscope (SEM) equipped with a field emission gun and a secondary electron detector (Nova NanoSEM 200 FEI Europe Company, accelerating voltage 10-15 kV, spot 4) coupled with an energy dispersion X-ray (EDX) analyser with a SiLi detector (EDAX, Netherlands) in the low vacuum mode. Cross sections were prepared by hydrogel cutting with a scalpel blade. Materials were analysed after coating with a carbon layer.

Architecture of crosslinked hydrogels were evaluated using micro-computed tomography (µ-CT) using a SkyScan 1272 equipment high-resolution X-ray microtomograph (Bruker Micro-CT, Belgium). 2D projections were registered averaging 3 frames, rotation of 0.3° and 800 ms exposure time. The images were registered at a resolution of 4904 x 3280 at an accelerating voltage of 50 kV and a beam current of 200 µA. The pixel size was fixed at 2 µm.

2.3. Mechanical analysis

Mechanical strength of the hydrogels was determined using an Inspekt 5 Table Blue testing machine (Hegewald & Peschke, Germany) equipped with a 100 N load cell. Samples were cut into cylinders of 10 mm height and compressed with a displacement rate of 5 mm min^{-1} (n = 10). Subsequently, Young's modulus (E_C) and the stresses corresponding to compression of a sample by 50% ($\sigma_{50\%}$) were measured. The results were expressed as mean ± standard deviation (SD).

2.4. Thermal analysis

Thermogravimetric analysis (TGA) was performed using a Discovery TGA 550 analyser (TA Instruments, USA) in the temperature range from 40 to 600 °C at a heating rate of 10 °C min^{-1}, under a nitrogen atmosphere. The samples (c.a. 15 mg) were placed in a platinum crucible.

2.5. FTIR analysis

The attenuated total reflection Fourier transform infrared (ATR-FTIR) spectra were registered using Vertex 70v spectrometer (Bruker, USA) equipped with a ZnSe ATR crystal. Spectra were collected in the 550-4000 cm^{-1} spectral range with a resolution of 4 cm^{-1} and by averaging 128 scans.

2.6. XPS analysis

X-ray photoelectron spectroscopy (XPS) analysis was performed in an ultrahigh vacuum system ($5 \cdot 10^{-9}$ mbar) equipped with an SES R4000 analyser (Gammadata Scienta, Sweden).

A monochromatic Al Kα X-ray source (1486.6 eV) was used. The electron binding energy of C1s peak was referenced at 284.8 eV. The obtained XPS spectra were analysed using CasaXPS 2.3.15 software.

2.7. Swelling and degradation studies

Swelling and degradation behaviour of hydrogels was investigated by incubating the samples (n = 5) in phosphate buffered saline (PBS, pH 7.4) at 37 °C. For swelling tests, the samples were weighed at the beginning of the experiment and again after 3 h, 1, 3, 7, and 14 days of incubation. Before weighing the samples were placed on filter paper to remove excess PBS from the surface. Swelling of each sample was calculated as follows: $\frac{W_t - W_0}{W_0} \times 100\%$, where W_t is weight after specific period of incubation, W_0 is weight before incubation. For degradation tests, the samples were weighed at the beginning of the experiment and again after 3, 7, and 14 days of incubation after freeze-drying. Mass loss of each sample was calculated as follows: $\frac{W_0 - W_t}{W_0} \times 100\%$, where W_0 is the weight of the sample before incubation and W_t is the weight of the freeze-dried sample after a specific period of incubation. The results were expressed as mean ± standard deviation (SD).

2.8. Antioxidant activity and release of THBA and RA

Antioxidant activity of the hydrogels was evaluated using ABTS and DPPH free radical scavenging assays and ferric reducing antioxidant power (FRAP) test (Dziadek, Dziadek, et al., 2021). The samples were incubated with shaking in ABTS, DPPH, and FRAP working solutions for 10 minutes in the dark at 30 ºC (n = 3). For ABTS, DPPH, and FRAP assays, the changes of absorbance at 734 nm, 515 nm, and 593 nm respectively, were measured using a spectrometer (UV-1800, RayLeigh, China). The radical scavenging capacity (RSC) of the materials was calculated as follows: $RSC = \frac{A_0 - A_S}{A_0} \times 100\%$, where A_S was the absorbance of the solution after sample incubation, and A_0 was the absorbance of ABTS and DPPH working solutions. The results of the FRAP test were expressed as absorbance. The results were expressed as mean ± standard deviation (SD).

The release of THBA and RA from hydrogels to PBS was evaluated using HPLC. A Prominence-i LC-2030C 3D Plus system (Shimadzu, Japan) equipped with a diode array detector (DAD) was used. The separation was performed on the Luna Omega 5 µm Polar C18, 100 A, 250 x 10 mm column (Phenomenex, California, USA) at 40ºC. The mobile phase was a mixture of two eluents: A – 0.1 % v/v formic acid in UHQ water and B – 0.1 % v/v formic acid in methanol. The flow rate of the mobile phase was 1.2 mL min^{-1}. The analysis was carried out

with the following gradient conditions: from 20% to 40% B in 10 min, 40% B for 10 min, from 40% to 50% B in 10 min, from 50% to 60% B in 5 min, 60% B for 5 min, from 60% to 70% B in 5 min, from 70% to 90% B in 5 min, 90% B for 5 min, from 90% to 20% B (the initial condition) in 1 min and 20% B for 4 min, resulting in a total run time of 60 min. The injection volume was 20 µL. All of the reagents used for HPLC analysis were purchased from Sigma-Aldrich, Germany.

2.9. *In vitro* mineralisation studies

The mineralization process of hydrogels was performed by incubation in simulated body fluid (SBF), prepared according to Kokubo and Takadama (Kokubo & Takadama, 2006). Samples were incubated in SBF for 7 and 14 days at 37 ℃, freeze-dried and analysed using SEM/EDX and ATR-FTIR methods as mentioned above.

2.10. *In vitro* cell studies

The human normal skin fibroblasts (BJ, ATCC, USA) and the human colon cancer epithelial cells (HT-29, ATCC, USA) were cultured in direct contact with crosslinked materials in Eagle's Minimum Essential Medium (EMEM, Sigma-Aldrich, MO, USA) and McCoy's 5a Medium Modified (ATCC, USA), respectively, both containing 10% Fetal Bovine Serum (FBS) at a density of $2 \cdot 10^4$ cells/mL/well for 1, 3, 7, and 10 days in 48-well plates. The bottom surfaces of tissue culture polystyrene (TCPS) wells served as a control. The proliferation rate of cells and cytotoxicity of hydrogels were assessed using the ToxiLight™ BioAssay Kit and ToxiLight™ 100% Lysis Reagent Set (Lonza, USA) according to the manufacturer's protocol. The kit was used to quantify adenylate kinase in both supernatant (representing damaged cells) and lysate (representing intact adherent cells). The results were expressed as mean ± standard deviation (SD) from 4 samples for each experimental group.

2.11. Statistical analysis

The results were analyzed using one-way analysis of variance (ANOVA) with Duncan post hoc tests, which were performed with Statistica 13 (StatSoft®, USA) software. The results were considered statistically significant when $p<0.05$.

3. Results and discussion

The use of monoaldehydes as crosslinking agents of chitosan is not as common as the use of other ones, e.g. glutaraldehyde. However, due to their natural origin, low cytotoxicity, low costs, and therapeutic activity, they have attracted great attention for crosslinking chitosan hydrogels for biomedical applications. To date, the following monoaldehydes have been used - vanillin (Hu et al., 2021; Karakurt et al., 2021; Xu et al., 2018), salicylaldehyde (Iftime et al.,

2017, 2020), nitrosalicylaldehyde (Craciun et al., 2019; Olaru et al., 2018), and cinnamaldehyde (Marin et al., 2014). In most cases, single-component hydrogels were obtained. However, there are only a few reports on the introduction of functional components into imine-chitosan hydrogels and examination of their effect on the crosslinking process, and thus the final properties of materials. In recent works, melt-derived bioactive glass particles (Hu et al., 2021) and diclofenac sodium salt (Craciun et al., 2019; Iftime et al., 2020), as a model drug, were used. In the present study we developed multicomponent chitosan-based hydrogels modified with a second hydrogel-forming polymer - pectin, as well as different functional additives – bioactive glass particles and rosmarinic acid. For systematic evaluation of the obtained hydrogels, the additives were introduced alone or in combination to both materials prepared in the presence and absence of monoaldehyde (THBA, pyrogallolaldehyde). It is worth mentioning that the THBA molecule contains three hydroxyl groups which, in addition to their ability to stabilize the imine bond, provided additional binding sides for the chains of both polymers and other components. Importantly, these three hydroxyl groups impart antioxidant properties to the THBA. Pectin was able to form polyelectrolyte complexes with chitosan through electrostatic interactions between ionised moieties. The BG particles used, similarly to RA, also contain numerous hydroxyl groups capable of forming hydrogen bonds. Furthermore, calcium ions, massively released from BG particles, were involved in ionic crosslinking of pectin. All of these reactions and interactions provided a multi-level crosslinking effect of chitosan-based hydrogels, as was schematically illustrated in **Fig. 2**, affecting their properties discussed in the next subsections.

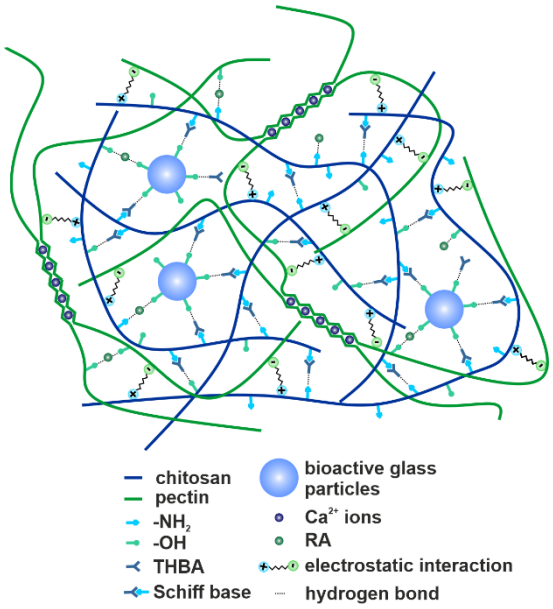

Figure 2. Schematic illustration of the network of THBA-containing CS-PC/A2/RA hydrogel.

3.1. Microstructure analysis

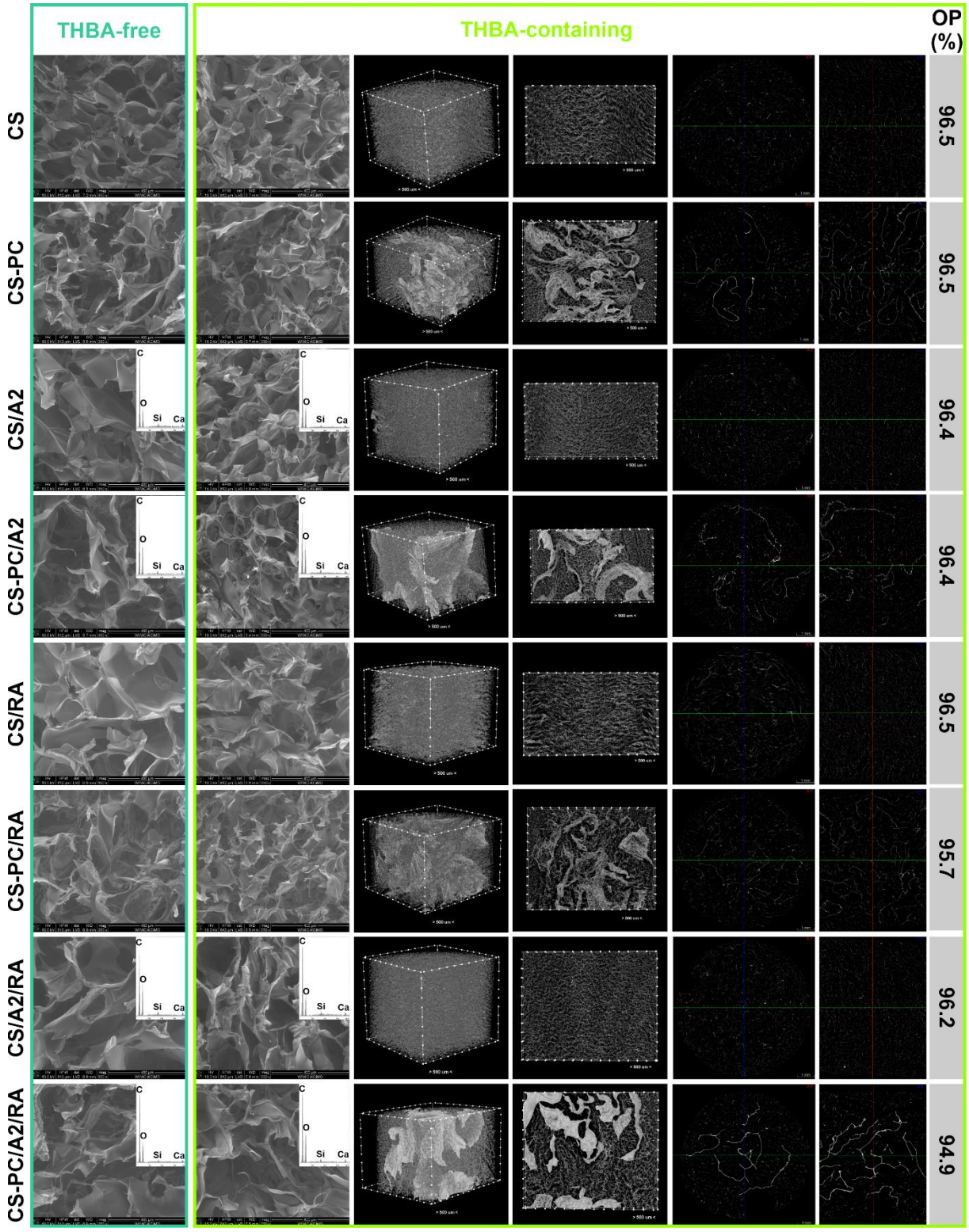

Figure 3. Representative SEM images and EDX spectra of the THBA-free and THBA-containing hydrogels. Representative μCT analyses of the crosslinked hydrogels - 3D reconstructions, cross sections, and open porosity (OP).

SEM analysis of hydrogels revealed irregular highly porous morphology characteristic of biopolymer-based porous materials obtained using freeze-drying processes (**Fig. 3**) (Coimbra et al., 2011; Luppi et al., 2010). All materials showed sheet/sponge-like structures. Additionally, the hydrogels with pectin contained fibrous-like structures, observed also by Coimbra et al., 2011 and Luppi et al., 2010 in CS-PC porous materials. Pores of crosslinked materials seemed be smaller compared to uncrosslinked hydrogels. This may be due to lower amounts of water entrapped between crosslinked chitosan chains (Iftime et al., 2017), which was confirmed by TG analysis (**Fig. A.4**). Although BG particles are not clearly visible in SEM and µCT analyses, the main components of BG (Si, Ca) were detected using EDX analysis, confirming their presence in the hydrogel matrices. This may be related to the low concentration of BG particles in materials (5 w/w%) and their highly homogeneous distribution with no tendency to agglomerate.

µCT analysis of crosslinked hydrogels proved nearly 100% interconnectivity of the pores and high porosity, regardless of the composition of the hydrogels. Open porosity was in the range of 94.9% – 96.5% (**Fig. 3**). The analysis of pore size distribution showed that all hydrogels had pores predominantly in the range of 50-150 µm (**Fig. 4A**), which is consistent with SEM observations (**Fig. 3**). Smaller (2-50 µm) and larger (>150 µm) pores were also present, as depicted by **Fig. 4A**. Such multi-scale pore size distribution, high porosity and interconnectivity promote migration and proliferation of osteogenic cells, vascularization, transport of nutrients and waste, as well as bone tissue ingrowth (Iviglia et al., 2016). Wall thickness was predominantly in the range of 2-18 µm (**Fig. 4B**). 3D reconstructions and cross sections obtained from µCT analysis revealed that CS-based materials had homogenous porous morphology. In the case of CS-PC-based hydrogels, two phases differing in microstructure were observed. Within the most porous phase, similar to that observed in CS-based materials, an inhomogenously distributed and significantly less porous second phase was noted. The latter was possibly PC and/or PC-CS PEC. Inhomogeneous distribution of the PC-containing phase probably results from immediate electrostatic interactions between pectin and chitosan during material preparation. This may also explain the lack of aforementioned agglomeration of BG. This was in contrast to our previous observations made for injectable PC/BG hydrogels, in which non-uniformly distributed agglomerates of A2 BG particles were noted, as a result of extremely rapid local crosslinking process of pectin induced by Ca^{2+} ions released from BG (Douglas et al., 2019). It should be pointed out that during hydrogel preparation, PC solution was added after mixing BG suspension with chitosan solution. As both calcium-induced

crosslinking of pectin and formation of PEC are competitive processes, the order in which the components were mixed favours the latter process, preventing BG agglomeration.

To date, μCT techniques have been used to investigate hydrogel microstructure and distribution of inorganic particles in hydrogel matrices (Douglas et al., 2019; Dziadek, Charuza, et al., 2021; Dziadek et al., 2019). However, our results clearly indicate that μCT imaging is also useful tool to study homogeneity and interactions in hydrogel polyelectrolyte complex matrices formed between polyanions and polycations, i.e. chitosan and pectin.

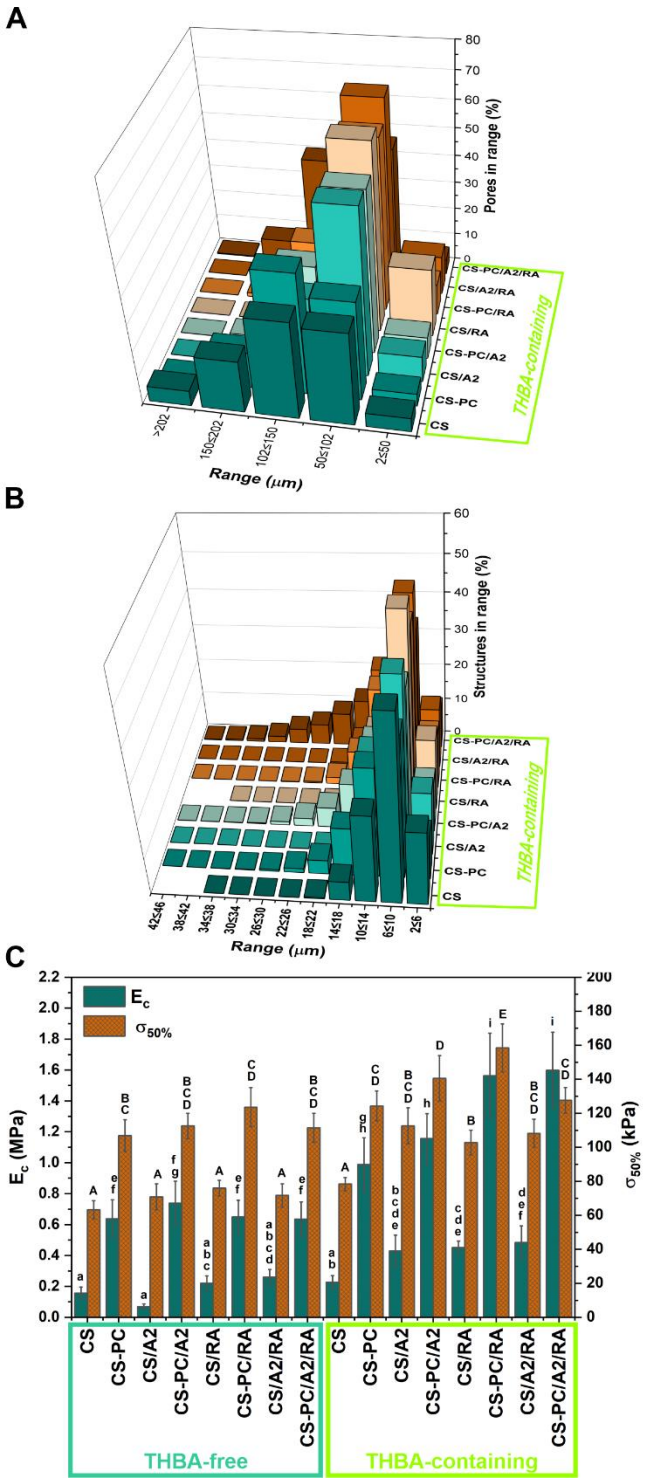

Figure 4. Quantitative data based on μCT analyses of the THBA-containing hydrogels: pore size distribution (A) and structure size distribution (B). Compression test results: Young's modulus and stresses corresponding to compression of a sample by 50% of the THBA-free and THBA-containing hydrogels (C). Statistically significant differences ($p < 0.05$) between materials are indicated by subsequent lower (E_C) and upper ($\sigma_{50\%}$) Latin letters. Different letters indicate statistically significant differences.

3.2. Mechanical analysis

As shown in **Fig. 4C**, hydrogels crosslinked with THBA exhibited significantly higher values of E_c and $\sigma_{50\%}$ (0.22-1.60 MPa and 78-158 kPa, respectively) compared to materials without THBA (0.07-0.73 MPa and 63-123 kPa, respectively). In turn, the presence of pectin in both THBA-containing and THBA-free materials led to significant increases in E_c and $\sigma_{50\%}$ (0.64-1.60 MPa and 106-158 kPa, respectively), when comparing to materials without PC (0.07-0.48 MPa and 63-113 kPa, respectively). Interestingly, improved mechanical properties were observed despite an uneven distribution of the PC-containing phase. However, because of its lower porosity, this phase may be considered as a reinforcing element of a highly porous hydrogel matrix. In the group of materials crosslinked with THBA, the presence of each additive resulted in higher values of both parameters tested. However, the highest E_c values were showed by CS-PC-based hydrogels modified with RA (CS-PC/RA, 1.56 MPa) as well as with both RA and BG (CS-PC/A2/RA, 1.60 MPa), while the highest $\sigma_{50\%}$ value was noted for the first mentioned one (CS-PC/RA, 158 kPa).

Crosslinking has been shown to be an effective strategy to enhance the mechanical properties of biopolymers as a result of formation of a three-dimensional polymer network (Martínez et al., 2015). Xu et al., 2018 showed that the formation of Schiff base bond/hydrogen bond linkage in chitosan hydrogels crosslinked with vanillin provide good mechanical strength and additional self-healing properties. The effect of interactions occurring between chitosan and pectin chains (electrostatic, ion-dipole interactions and hydrogen bonding) on improvement of mechanical properties of porous CS/PC materials was previously observed (Demir et al., 2020). In turn, Chen et al., 2010 showed that the presence of Ca^{2+} ions in a CS-PC PEC membrane significantly improved its tensile strength, because of additional calcium-mediated ionic interactions between pectin chains. In recent work, BG particles were considered as a co-crosslinker, improving mechanical behaviour of CS/BG/vanillin hydrogels. BG particles provided additional binding sites between chitosan and vanillin through multiple hydrogen bonding (Hu et al., 2021). Taking together, the improved mechanical properties of the obtained multicomponent scaffolds could be attributed to the higher crosslinking degree promoted by multifaceted interactions between components.

Formation of the Schiff base in the chitosan matrix was confirmed by development of a distinct yellow colour (**Fig. 5C**) (Stroescu et al., 2015). The FTIR spectra of THBS-containing hydrogels showed an absorption band at 1628 cm^{-1}, which may be attributed to the stretching vibration of imine bonding (**Fig. A.2**). Furthermore, an absorption band of the phenolic hydroxyl groups of THBA shifted from 1279 to 1268 cm^{-1}, which may be due to the H-bonding

between THBA and other components (Y. Zhang et al., 2014). The high-resolution C1s and N1s XPS spectra of the THBA-containing CS hydrogel revealed peaks at 288.8 eV and 398.8 eV (**Fig. A.3**), respectively, which can be assigned to the binding energy of the C=N bond (Gao et al., 2021), suggesting that a Schiff base reaction occurred. When analysing the TG curves, crosslinked materials showed lower water content (lower initial weight loss up to 200 ℃) as well as enhanced thermal stability (higher temperature of thermal decomposition, occurring between 200 and 350 ℃, and higher residual weight) compared to uncrosslinked hydrogels, confirming the presence of covalent Schiff base bonding (**Fig. A.4**) (Montaser et al., 2019). Moreover, in the case of uncrosslinked materials, temperature of thermal decomposition of CS-PC hydrogels tended to be higher compared to CS materials, which may indicate ionic interactions between both polymers (Martins et al., 2018).

3.3. Swelling and degradation studies

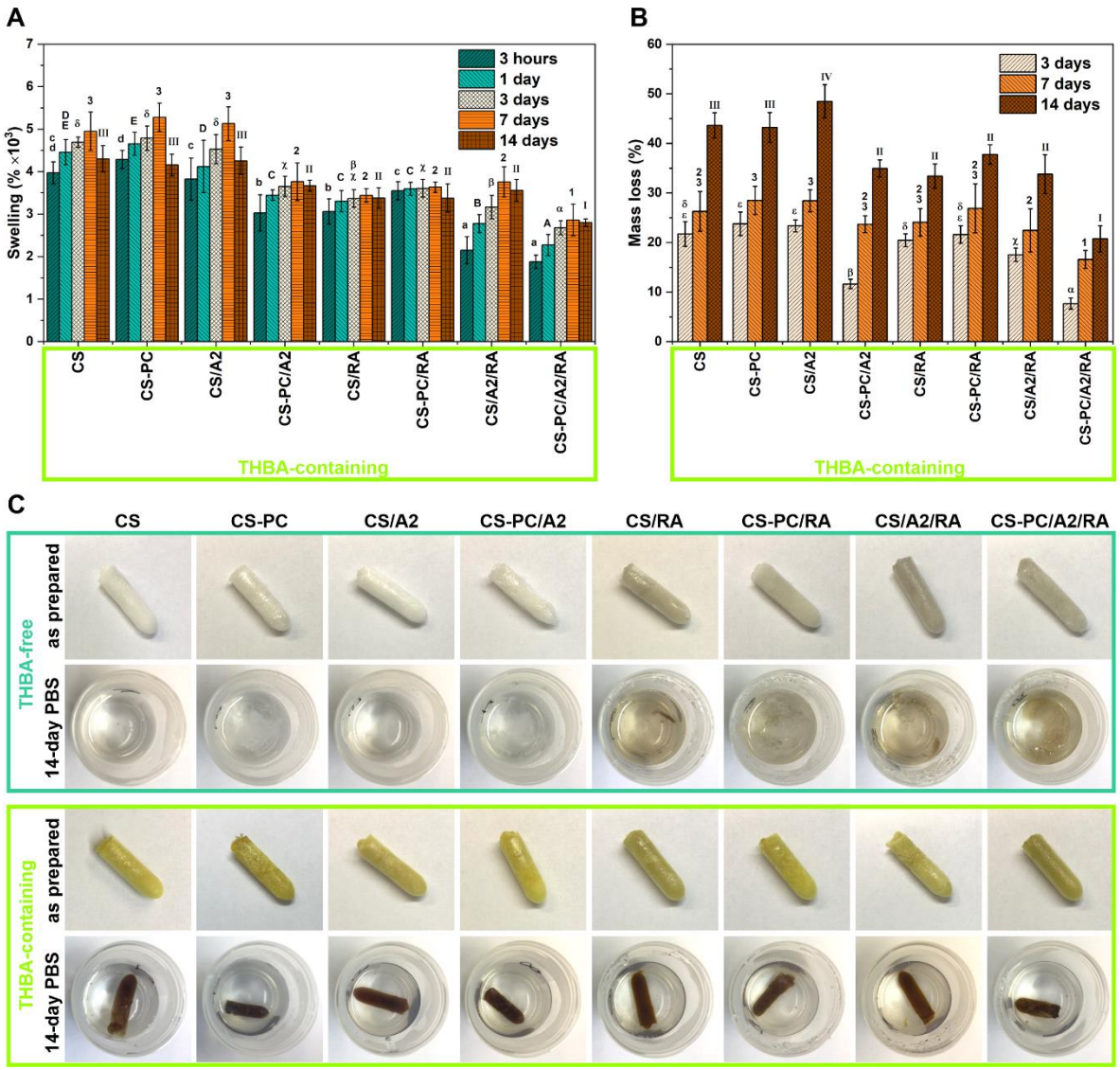

Figure 5. Swelling (A) and mass loss (B) of the THBA-containing hydrogels. Statistically significant differences ($p < 0.05$) between materials are indicated by subsequent lower (3 hours), upper (1 day) Latin letters, Greek letters (3 days), Arabic numerals (7 days), and Roman numerals (14 days). Different letters/numerals indicate statistically significant differences. Macroscopic images of the THBA-free and THBA-containing hydrogels before (as prepared) and after 14-day incubation in PBS (C).

Swelling and degradation behaviour of hydrogels crosslinked with THBA was investigated, because only these ones were able to maintain a sufficient integrity for accurate weighing (**Fig. 5C**). Materials swelled the most after the first 3 hours of incubation in PBS (1878-4287%). Swelling ability of all THBA-containing materials gradually increased with increasing incubation time until day 7 (**Fig. 5A**). After 14 days of incubation, a decrease in swelling was observed, which suggests that the dissolution process was accelerated. This is in agreement with the highest mass loss of hydrogels after 14-day incubation (**Fig. 5B**). Hydrogels containing RA and CS-PC/A2 material exhibited a lower decrease in swelling and lower mass loss after 14-day incubation compared to other materials. Furthermore, significantly lower water uptake and mass loss over the entire incubation period were observed for these materials. When comparing hydrogels with pectin, those ones modified with BG particles showed significantly reduced swelling and degradation. Importantly, materials combining all components (CS, PC, THBA, RA, BG) were the most stable.

Macroscopic observations showed that the materials crosslinked with THBA maintained shape and integrity over the entire incubation period. The THBA-free hydrogels containing pectin did not dissolve completely during 14-day incubation in PBS, in contrast to materials without this component (**Fig. 5C**). Also, hydrogels with RA exhibited incomplete dissolution in PBS, however debris were much smaller after 14-day incubation compared to materials with PC. THBA-free CS-PC/A2/RA hydrogel showed the lowest tendency to disintegrate/dissolve with a very high swelling rate.

Both swelling and degradation behaviour of hydrogels strongly depend on the degree of crosslinking and also the nature of linkage. In general, the higher the crosslinking degree, the lower the swelling ability and the slower the degradation rate (Hu et al., 2021; Iftime et al., 2017). Therefore, the results clearly indicated that THBA was successfully used as a crosslinking agent of CS-based hydrogels. The presence of PC, RA, and BG in THBA-free materials also induced crosslinking, but this effect was much weaker. This was due to the fact that the covalent bonding (Schiff base bond) is known to be much stronger than ionic

interactions (calcium-mediated interactions between PC chains and interactions between ionised functional groups of CS and PC) as well as hydrogen bonding (e.g. between hydroxyl groups of RA, BG, CS, and PC). The introduction of PC, RA, and BG into THBA-containing hydrogels gave a synergistic crosslinking effect.

Pornpimon and Sakamon (Pornpimon & Sakamon, 2010) showed that swelling of the chitosan films was reduced upon modification with the plant extract rich in polyphenols, as a result of intermolecular interactions between chitosan and the extract components. In contrast, literature data showed that the swelling ability and degradation rate of CS-based materials crosslinked with glutaraldehyde considerably increased upon addition of PC (Demir et al., 2020), while the presence of Ca^{2+} ions in CS-PC PEC materials accelerated the weight loss during incubation in PBS (Chen et al., 2010). It seems that THBA provided a stabilizing effect in CS-PC hydrogels, due to the hydrogen bonds established between the hydroxyl groups of THBA and pectin moieties. Furthermore, because of the lower content of pectin with respect to chitosan, PC-containing phase may be entrapped between highly crosslinked CS phases, creating a protective environment against water. This can be supported by µCT analysis (**Fig. 3**).

3.4. Antioxidant activity and release of biologically active compounds

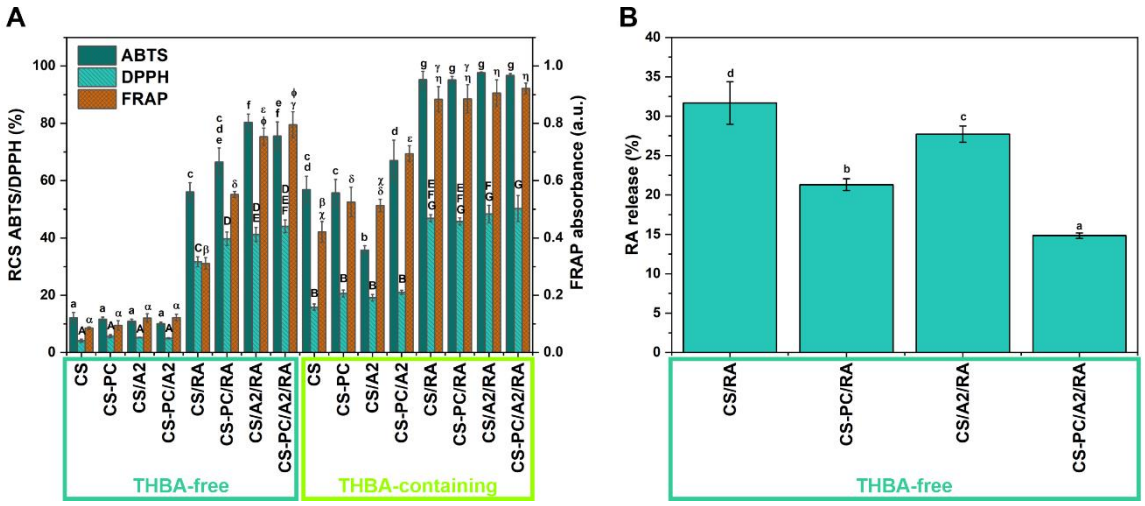

Figure 6. Radical scavenging capacity (RSC) against the $ABTS^{\bullet+}$ and $DPPH^{\bullet}$ radicals, as well as ferric reducing antioxidant potential (FRAP) of the THBA-free and THBA-containing hydrogels (A). Statistically significant differences ($p < 0.05$) are indicated by subsequent lower (ABTS), upper (DPPH) Latin letters and Greek letters (FRAP). The release of RA to PBS after 14-day incubation - % of the initial content in the materials (B). Statistically significant differences ($p < 0.05$) are indicated by subsequent lower Latin letters. Different letters indicate statistically significant differences.

The radical scavenging capacity (RSC) against the $ABTS^{\bullet+}$ and $DPPH^{\bullet}$ radicals, as well as the ferric reducing antioxidant potential (FRAP) of the hydrogels, are shown in **Fig. 6A**. Antioxidant activity of hydrogels can be clearly ascribed to the presence of phenolic components – THBA and RA. The materials containing these components showed high RSC and reducing potential which increased in the following order: THBA<RA<THBA+RA. In the case of materials with both THBA and RA, antioxidant potential did not depend on composition, in contrast to hydrogels with a single phenolic component (THBA or RA).

The release of biologically active compounds form hydrogels was evaluated after 14-day incubation in PBS (**Fig. 6B**). The release of THBA and RA form hydrogels crosslinked with THBA was below 1% of the initial content in the materials (data not shown). In the case of THBA-free hydrogels, release of RA was in the range 21% – 32%, depending on material composition. The presence of PC and BG separately decreased RA release significantly, while combination of these components (PC and BG) reduced RA release to the greatest extent. The release of RA from THBA-free hydrogels corresponded to yellowish colour of incubation medium (**Fig. 5C**).

A very low release level of THBA from THBA-containing hydrogels indicated its strong interactions with other components of the materials, confirming contribution in crosslinking process. Crosslinking with THBA inhibited almost completely the release of RA. In the case of THBA-free materials, RA release level corresponded with swelling/dissolution rate of the hydrogels (evaluated macroscopically – **Fig. 5C**). This indicates that, besides the interaction of RA with hydrogel components, the crosslinking process using THBA enables RA to be effectively entrapped in the hydrogel network. This is in agreement with other studies indicating that reduced release of biologically active components from the hydrogel is closely correlated with a higher degree of crosslinking and therefore lower swelling and degradation rates (Iftime et al., 2020; Karakurt et al., 2021).

Although THBA and RA were practically not released from the hydrogels crosslinked with THBA, they showed high antioxidant activity. Furthermore, the release level of RA from THBA-free hydrogels did not correlate with RSC and reducing potential. This may indicate that antioxidant activity of hydrogels is mainly attributed to antioxidants attached to the materials, not to the released ones (Dziadek, Dziadek, et al., 2021). Some differences in antioxidant activity between hydrogels containing a single phenolic compound (THBA or RA) may result from different interactions between them and other components (CS, PC, BG). As the antioxidant activity of a phenolic compound depends on the total number of phenolic hydroxyl

groups able to interact with reactive oxygen species by donating hydrogens, phenolic hydroxyl groups involved in hydrogen bonding were not available to scavenge free radicals/reduce ferric ions. In turn, the combination of both THBA and RA provided maximal antioxidant effect.

3.5. *In vitro* mineralisation studies

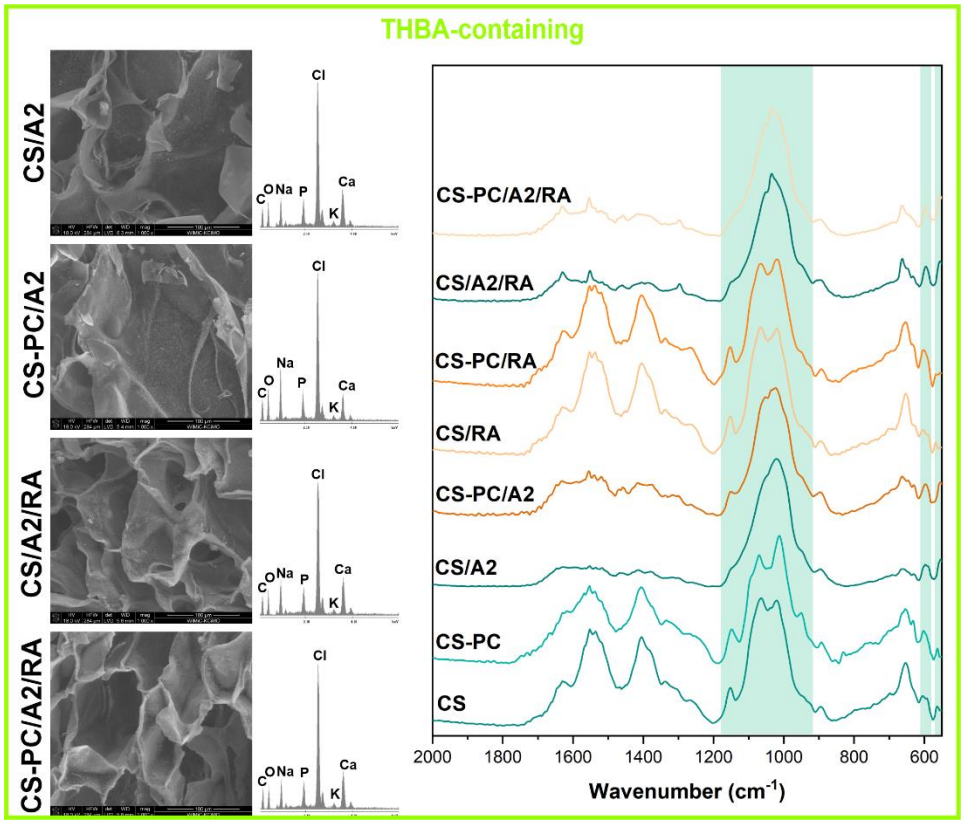

Figure 7. SEM images, EDX spectra, and ATR-FTIR spectra of the THBA-containing hydrogels after 14-day incubation in SBF.

Mineralisation process of the THBA-containing hydrogels after incubation in SBF was assessed using SEM/EDX and ATR-FTIR methods (**Fig. 7**). After 14-day incubation, hydrogels containing BG particles were covered with a uniform layer rich in calcium (Ca) and phosphorus (P). Furthermore, quite large amounts of sodium (Na), chlorine (Cl), and potassium (K) were incorporated into materials from SBF. In the case of crosslinked hydrogels without BG, only the latter elements (Na, Cl, K) were detected after incubation (data not shown). ATR-FTIR spectra of hydrogels containing BG particles incubated in SBF releveled new bands proving mineralisation by a CaP phase. Furthermore, the reduction in the intensity of bands arising from hydrogels was observed, indicating that the layer was thick and uniformly covered the materials. The bands noted in the ranges of 960 - 1130 cm^{-1} and 600 - 560 cm^{-1} correspond to

stretching and bending vibrations of PO_4^{3-} groups in crystalline CaP, respectively (Bossard et al., 2019). The bands in spectra of hydrogels containing RA tended to be sharper, compared to those without RA, suggesting the presence of CaP phase with higher crystallinity. This may be due to acceleration of CaP layer crystallization by additional polyphenolic compound with numerous phenolic hydroxyl groups capable to interact with Ca^{2+} ions from SBF (Zhou et al., 2012). There were no significant changes in the spectra of THBA-containing hydrogels without BG after incubation, confirming SEM/EDX analysis.

These results confirmed the mineralisation ability of CS- and CS-PC-based hydrogels containing BG particles. This may provide chemical bonding with bone, as well as improved mechanical properties of the hydrogels after implantation, actively promoting bone regeneration (Mota et al., 2012).

3.6. *In vitro* cell studies

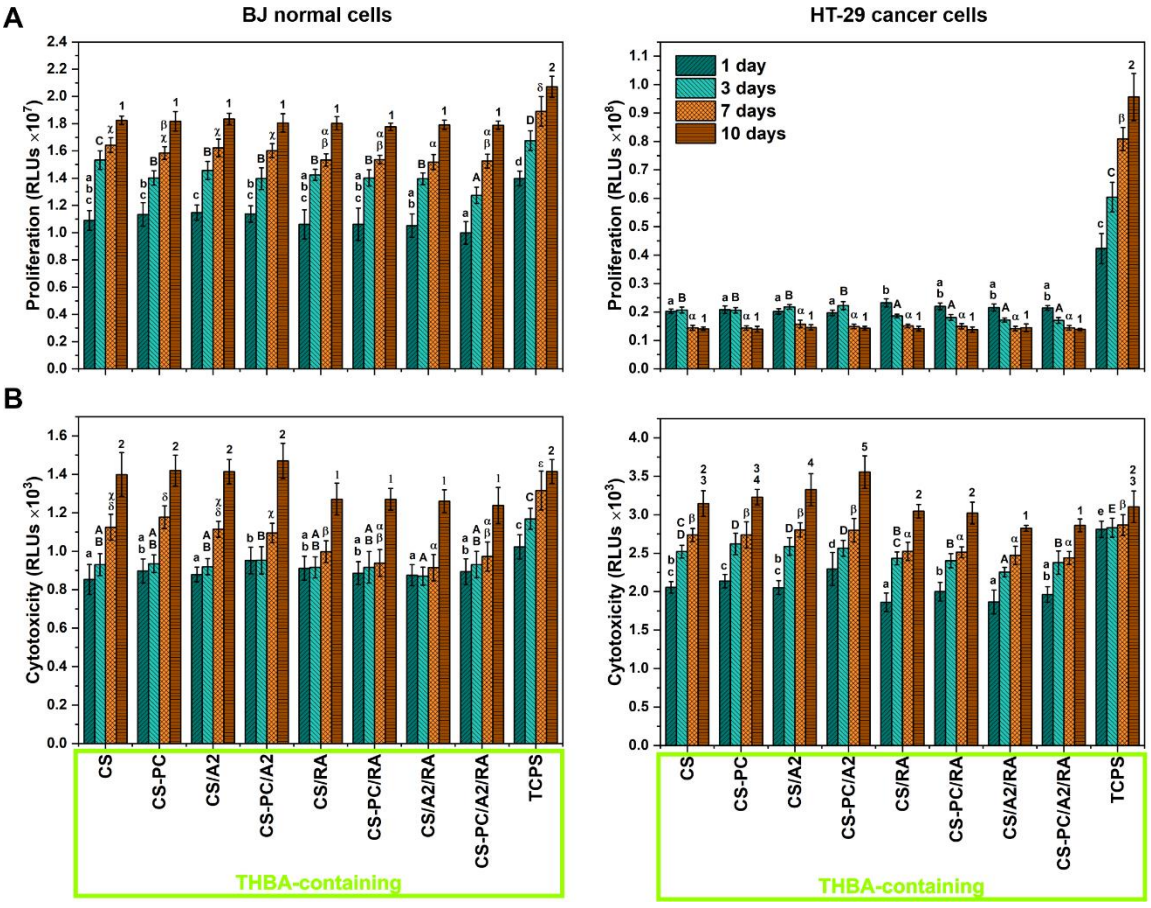

Figure 8. The response of BJ human normal skin fibroblasts and HT-29 human colon cancer epithelial cells cultured in contact with THBA-containing hydrogels: adenylate kinase (AK) level in the lysate corresponding to the number of intact adherent cells (A), AK level in the

supernatant representing material cytotoxicity (B). Statistically significant differences ($p < 0.05$) between materials and TCPS are indicated by subsequent lower (1 day), upper (3 days) Latin letters, Greek letters (7 days), Arabic numerals (10 days). Different letters indicate statistically significant differences.

Cytotoxicity and antiproliferative activity of THBA-containing hydrogels were evaluated on normal fibroblast cells and colon cancer cells (**Fig. 8**). The number of normal cells in contact with tested materials was lower after each cell culture period compared to the control (TCPS). Nevertheless, the fibroblasts cultured on hydrogels showed a high proliferation rate. After 10 days of culture, there were no statistically significant difference between materials. In the case of cancer cells, a strong antiproliferative activity of the materials was noted. The number of cancer cells in contact with the hydrogels was several times lower compared to TCPS and decreased with increasing culture time. In the case of materials containing RA, a significantly lower number of cells was observed after 3 days of culture, compared to hydrogels without RA. In turn, after 10-day culture, the number of cells in contact with materials did not differ significantly. Release of adenylate kinase from both normal and cancer cells in contact with hydrogels was on the same level or even lower compared to the control, indicating a low cytotoxic effect. Materials containing RA showed lower cytotoxicity when compared to unmodified ones.

The results showed that materials crosslinked with THBA were not cytotoxic against normal and cancer cells, however they inhibited the proliferation of cancer cells, possibly indicating a modulation of the cell cycle. This suggested that apoptosis rather than necrosis was a pathway for cancer cell death. Inducing apoptosis of cancer cells while reducing the death of normal cells is one of the most desirable mechanisms of action of anticancer therapies (Kwan et al., 2015). Antiproliferative activity of THBA-containing hydrogels may be ascribed to the presence of phenolic compounds – THBA and RA. As mentioned above, monoaldehydes, such as vanillin (Karakurt et al., 2021), salicylaldehyde (Iftime et al., 2017), o-vanillin, and 2,4,6-trihydroxybenzaldehyde (Marton et al., 2016), as well as polyphenols, for instance RA (Swamy et al., 2018), exhibited antitumor activity against different types of cancer cells. Similarly to antioxidant properties, anticancer activity was possibly attributed mainly to compounds attached to materials.

4. Conclusions

In the present work, a series of highly porous chitosan-based hydrogels was prepared and comprehensively evaluated. A simple and green method for crosslinking with the use of monoaldehyde - 2,3,4-trihydroxybenzaldehyde was successfully applied. The hydrogels were modified with a second hydrogel-forming polymer – pectin, as well as different functional additives – bioactive glass particles and rosmarinic acid. All of these were involved in the crosslinking process of the hydrogels, while simultaneously modulating their properties or imparting completely new ones. The crosslinking process with THBA resulted in significantly improved mechanical properties, high swelling capacity and delayed degradation. In addition to the crosslinking function, THBA provided high antioxidant activity and also a selective antiproliferative effect on cancer cells with no cytotoxicity for normal cells. Hydrogels containing pectin showed significantly modified microstructure and enhanced mechanical strength, while the combination with bioactive glass particles gave improved stability in PBS. All hydrogels modified with bioactive glass particles exhibited the ability to mineralize in SBF. The addition of rosmarinic acid enhanced antioxidant and anticancer activities as well as promoting the mineralisation process. The results indicated that the obtained hydrogels represent promising multifunctional biomaterials with a wide range of tunable physicochemical and biological properties with great potential for the use in different tissue engineering fields, for instance in bone regeneration or after tumour resection.

5. Acknowledgments

This work was supported by the National Science Centre, Poland, grant nos. 2017/27/B/ST8/00195 (KCK) and 2019/32/C/ST5/00386 (MD). The µCT investigations were possible due to European Regional Development Fund through Competitiveness Operational Program 2014-2020, Priority axis 1, ID P_36_611, MySMIS code 107066, INOVABIOMED (AS, ICS). This work was partly supported by program „Excellence initiative – research university" for the AGH University of Science and Technology. The authors thank Herbstreith & Fox Company (Germany) for delivering pectin.

6. Literature

Birch, N. P., Barney, L. E., Pandres, E., Peyton, S. R., & Schiffman, J. D. (2015). Thermal-Responsive Behavior of a Cell Compatible Chitosan/Pectin Hydrogel. *Biomacromolecules*, *16*(6), 1837–1843. https://doi.org/10.1021/ACS.BIOMAC.5B00425

Bossard, C., Granel, H., Jallot, É., Montouillout, V., Fayon, F., Soulié, J., Drouet, C., Wittrant, Y., & Lao, J. (2019). Mechanism of Calcium Incorporation Inside Sol–Gel Silicate Bioactive Glass and the Advantage of Using Ca(OH)2 over Other Calcium

Sources. *ACS Biomaterials Science & Engineering*, *5*(11), 5906–5915. https://doi.org/10.1021/ACSBIOMATERIALS.9B01245

Chen, P. H., Kuo, T. Y., Kuo, J. Y., Tseng, Y. P., Wang, D. M., Lai, J. Y., & Hsieh, H. J. (2010). Novel chitosan–pectin composite membranes with enhanced strength, hydrophilicity and controllable disintegration. *Carbohydrate Polymers*, *82*(4), 1236–1242. https://doi.org/10.1016/J.CARBPOL.2010.06.057

Coimbra, P., Ferreira, P., de Sousa, H. C., Batista, P., Rodrigues, M. A., Correia, I. J., & Gil, M. H. (2011). Preparation and chemical and biological characterization of a pectin/chitosan polyelectrolyte complex scaffold for possible bone tissue engineering applications. *International Journal of Biological Macromolecules*, *48*(1), 112–118. https://doi.org/10.1016/J.IJBIOMAC.2010.10.006

Craciun, A. M., Mititelu Tartau, L., Pinteala, M., & Marin, L. (2019). Nitrosalicyl-imine-chitosan hydrogels based drug delivery systems for long term sustained release in local therapy. *Journal of Colloid and Interface Science*, *536*, 196–207. https://doi.org/10.1016/J.JCIS.2018.10.048

Cui, S., Yao, B., Gao, M., Sun, X., Gou, D., Hu, J., Zhou, Y., & Liu, Y. (2017). Effects of pectin structure and crosslinking method on the properties of crosslinked pectin nanofibers. *Carbohydrate Polymers*, *157*, 766–774. https://doi.org/10.1016/J.CARBPOL.2016.10.052

Demir, D., Ceylan, S., Göktürk, D., & Bölgen, N. (2020). Extraction of pectin from albedo of lemon peels for preparation of tissue engineering scaffolds. *Polymer Bulletin 2020 78:4*, *78*(4), 2211–2226. https://doi.org/10.1007/S00289-020-03208-1

Douglas, T. E. L., Dziadek, M., Schietse, J., Boone, M., Declercq, H. A., Coenye, T., Vanhoorne, V., Vervaet, C., Balcaen, L., Buchweitz, M., Vanhaecke, F., van Assche, F., Cholewa-Kowalska, K., & Skirtach, A. G. (2019). Pectin-bioactive glass self-gelling, injectable composites with high antibacterial activity. *Carbohydrate Polymers*, *205*, 427–436. https://doi.org/10.1016/J.CARBPOL.2018.10.061

Douglas, T. E. L., Kumari, S., Dziadek, K., Dziadek, M., Abalymov, A., Cools, P., Brackman, G., Coenye, T., Morent, R., Mohan, M. K., & Skirtach, A. G. (2017). Titanium surface functionalization with coatings of chitosan and polyphenol-rich plant extracts. *Materials Letters*, *196*, 213–216. https://doi.org/10.1016/J.MATLET.2017.03.065

Dziadek, M., Charuza, K., Kudlackova, R., Aveyard, J., D'Sa, R., Serafim, A., Stancu, I. C., Iovu, H., Kerns, J. G., Allinson, S., Dziadek, K., Szatkowski, P., Cholewa-Kowalska, K., Bacakova, L., Pamula, E., & Douglas, T. E. L. (2021). Modification of heat-induced whey protein isolate hydrogel with highly bioactive glass particles results in promising biomaterial for bone tissue engineering. *Materials & Design*, *205*, 109749. https://doi.org/10.1016/J.MATDES.2021.109749

Dziadek, M., Dziadek, K., Checinska, K., Zagrajczuk, B., Golda-Cepa, M., Brzychczy-Wloch, M., Menaszek, E., Kopec, A., & Cholewa-Kowalska, K. (2021). PCL and PCL/bioactive glass biomaterials as carriers for biologically active polyphenolic compounds: Comprehensive physicochemical and biological evaluation. *Bioactive Materials*, *6*(6), 1811–1826. https://doi.org/10.1016/J.BIOACTMAT.2020.11.025

Dziadek, M., Kudlackova, R., Zima, A., Slosarczyk, A., Ziabka, M., Jelen, P., Shkarina, S., Cecilia, A., Zuber, M., Baumbach, T., Surmeneva, M. A., Surmenev, R. A., Bacakova, L., Cholewa-Kowalska, K., & Douglas, T. E. L. (2019). Novel multicomponent organic–inorganic WPI/gelatin/CaP hydrogel composites for bone tissue engineering. *Journal of Biomedical Materials Research Part A*, *107*(11), 2479–2491. https://doi.org/10.1002/JBM.A.36754

Gao, C., Wang, S., Liu, B., Yao, S., Dai, Y., Zhou, L., Qin, C., & Fatehi, P. (2021). Sustainable Chitosan-Dialdehyde Cellulose Nanocrystal Film. *Materials 2021, Vol. 14, Page 5851*, *14*(19), 5851. https://doi.org/10.3390/MA14195851

Hu, J., Wang, Z., Miszuk, J. M., Zhu, M., Lansakara, T. I., Tivanski, A. v., Banas, J. A., & Sun, H. (2021). Vanillin-bioglass cross-linked 3D porous chitosan scaffolds with strong osteopromotive and antibacterial abilities for bone tissue engineering. *Carbohydrate Polymers*, *271*, 118440. https://doi.org/10.1016/J.CARBPOL.2021.118440

Iftime, M. M., Mititelu Tartau, L., & Marin, L. (2020). New formulations based on salicyl-imine-chitosan hydrogels for prolonged drug release. *International Journal of Biological Macromolecules*, *160*, 398–408. https://doi.org/10.1016/J.IJBIOMAC.2020.05.207

Iftime, M. M., Morariu, S., & Marin, L. (2017). Salicyl-imine-chitosan hydrogels: Supramolecular architecturing as a crosslinking method toward multifunctional hydrogels. *Carbohydrate Polymers*, *165*, 39–50. https://doi.org/10.1016/J.CARBPOL.2017.02.027

Iviglia, G., Cassinelli, C., Bollati, D., Baino, F., Torre, E., Morra, M., & Vitale-Brovarone, C. (2016). Engineered porous scaffolds for periprosthetic infection prevention. *Materials Science and Engineering: C*, *68*, 701–715. https://doi.org/10.1016/J.MSEC.2016.06.050

Karakurt, I., Ozaltin, K., Vargun, E., Kucerova, L., Suly, P., Harea, E., Minařík, A., Štěpánková, K., Lehocky, M., Humpolícek, P., Vesel, A., & Mozetic, M. (2021). Controlled release of enrofloxacin by vanillin-crosslinked chitosan-polyvinyl alcohol blends. *Materials Science and Engineering: C*, *126*, 112125. https://doi.org/10.1016/J.MSEC.2021.112125

Kokubo, T., & Takadama, H. (2006). How useful is SBF in predicting in vivo bone bioactivity? *Biomaterials*, *27*(15), 2907–2915. https://doi.org/10.1016/J.BIOMATERIALS.2006.01.017

Kuhlmann, A., & Röhl, C. (2008). Phenolic Antioxidant Compounds Produced by in Vitro. Cultures of Rosemary (Rosmarinus officinalis.) and Their Anti-inflammatory Effect on Lipopolysaccharide-Activated Microglia. *Http://Dx.Doi.Org/10.1080/13880200600794063*, *44*(6), 401–410. https://doi.org/10.1080/13880200600794063

Kwan, Y. P., Saito, T., Ibrahim, D., Al-Hassan, F. M. S., Oon, C. E., Chen, Y., Jothy, S. L., Kanwar, J. R., & Sasidharan, S. (2015). Evaluation of the cytotoxicity, cell-cycle arrest, and apoptotic induction by Euphorbia hirta in MCF-7 breast cancer cells. *Https://Doi.Org/10.3109/13880209.2015.1064451*, *54*(7), 1223–1236. https://doi.org/10.3109/13880209.2015.1064451

Lee, J.-W., Asai, M., Jeon, S.-K., Iimura, T., Yonezawa, T., Cha, B.-Y., Woo, J.-T., & Yamaguchi, A. (2015). Rosmarinic acid exerts an antiosteoporotic effect in the RANKL-induced mouse model of bone loss by promotion of osteoblastic differentiation and inhibition of osteoclastic differentiation. *Molecular Nutrition & Food Research*, *59*(3), 386–400. https://doi.org/10.1002/MNFR.201400164

Li, J., Zhu, D., Yin, J., Liu, Y., Yao, F., & Yao, K. (2010). Formation of nano-hydroxyapatite crystal in situ in chitosan–pectin polyelectrolyte complex network. *Materials Science and Engineering: C*, *30*(6), 795–803. https://doi.org/10.1016/J.MSEC.2010.03.011

Luppi, B., Bigucci, F., Abruzzo, A., Corace, G., Cerchiara, T., & Zecchi, V. (2010). Freeze-dried chitosan/pectin nasal inserts for antipsychotic drug delivery. *European Journal of Pharmaceutics and Biopharmaceutics*, *75*(3), 381–387. https://doi.org/10.1016/J.EJPB.2010.04.013

Maciel, V. B. v., Yoshida, C. M. P., & Franco, T. T. (2015). Chitosan/pectin polyelectrolyte complex as a pH indicator. *Carbohydrate Polymers*, *132*, 537–545. https://doi.org/10.1016/J.CARBPOL.2015.06.047

Mallick, S. P., Suman, D. K., Singh, B. N., Srivastava, P., Siddiqui, N., Yella, V. R., Madhual, A., & Vemuri, P. K. (2020). Strategies toward development of biodegradable hydrogels for biomedical applications. *Https://Doi.Org/10.1080/25740881.2020.1719135*, *59*(9), 911–927. https://doi.org/10.1080/25740881.2020.1719135

Marin, L., Moraru, S., Popescu, M. C., Nicolescu, A., Zgardan, C., Simionescu, B. C., & Barboiu, M. (2014). Out-of-Water Constitutional Self-Organization of Chitosan–Cinnamaldehyde Dynagels. *Chemistry – A European Journal*, *20*(16), 4814–4821. https://doi.org/10.1002/CHEM.201304714

Martínez, A., Blanco, M. D., Davidenko, N., & Cameron, R. E. (2015). Tailoring chitosan/collagen scaffolds for tissue engineering: Effect of composition and different crosslinking agents on scaffold properties. *Carbohydrate Polymers*, *132*, 606–619. https://doi.org/10.1016/J.CARBPOL.2015.06.084

Martins, J. G., de Oliveira, A. C., Garcia, P. S., Kipper, M. J., & Martins, A. F. (2018). Durable pectin/chitosan membranes with self-assembling, water resistance and enhanced mechanical properties. *Carbohydrate Polymers*, *188*, 136–142. https://doi.org/10.1016/J.CARBPOL.2018.01.112

Marton, A., Kúsz, E., Kolozsi, C., Tubak, V., Zagotto, G., Buzás, K., Quintieri, L., & Vizler, C. (2016). Vanillin analogues o-vanillin and 2,4,6-trihydroxybenzaldehyde inhibit NFκB activation and suppress growth of A375 human melanoma. *Anticancer Research*, *36*(11), 5743–5750. https://doi.org/10.21873/anticanres.11157

Montaser, A. S., Wassel, A. R., & Al-Shaye'a, O. N. (2019). Synthesis, characterization and antimicrobial activity of Schiff bases from chitosan and salicylaldehyde/TiO2 nanocomposite membrane. *International Journal of Biological Macromolecules*, *124*, 802–809. https://doi.org/10.1016/J.IJBIOMAC.2018.11.229

Mota, J., Yu, N., Caridade, S. G., Luz, G. M., Gomes, M. E., Reis, R. L., Jansen, J. A., Frank Walboomers, X., & Mano, J. F. (2012). Chitosan/bioactive glass nanoparticle composite membranes for periodontal regeneration. *Acta Biomaterialia*, *8*(11), 4173–4180. https://doi.org/10.1016/J.ACTBIO.2012.06.040

Munarin, F., Guerreiro, S. G., Grellier, M. A., Tanzi, M. C., Barbosa, M. A., Petrini, P., & Granja, P. L. (2011). Pectin-Based Injectable Biomaterials for Bone Tissue Engineering. *Biomacromolecules*, *12*(3), 568–577. https://doi.org/10.1021/BM101110X

Neufeld, L., & Bianco-Peled, H. (2017). Pectin–chitosan physical hydrogels as potential drug delivery vehicles. *International Journal of Biological Macromolecules*, *101*, 852–861. https://doi.org/10.1016/J.IJBIOMAC.2017.03.167

Neves, S. C., Gomes, D. B., Sousa, A., Bidarra, S. J., Petrini, P., Moroni, L., Barrias, C. C., & Granja, P. L. (2015). Biofunctionalized pectin hydrogels as 3D cellular microenvironments. *Journal of Materials Chemistry B*, *3*(10), 2096–2108. https://doi.org/10.1039/C4TB00885E

Olaru, A. M., Marin, L., Morariu, S., Pricope, G., Pinteala, M., & Tartau-Mititelu, L. (2018). Biocompatible chitosan based hydrogels for potential application in local tumour therapy. *Carbohydrate Polymers*, *179*, 59–70. https://doi.org/10.1016/J.CARBPOL.2017.09.066

Pornpimon, M., & Sakamon, D. (2010). Effects of drying methods and conditions on release characteristics of edible chitosan films enriched with Indian gooseberry extract. *Food Chemistry*, *118*(3), 594–601. https://doi.org/10.1016/J.FOODCHEM.2009.05.027

Sitarz, M., Bulat, K., Wajda, A., & Szumera, M. (2013). Direct crystallization of silicate-phosphate glasses of NaCaPO 4-SiO2 system. *Journal of Thermal Analysis and Calorimetry*, *113*(3), 1363–1368. https://doi.org/10.1007/S10973-013-3240-Y/FIGURES/7

Stroescu, M., Stoica-Guzun, A., Isopencu, G., Jinga, S. I., Parvulescu, O., Dobre, T., & Vasilescu, M. (2015). Chitosan-vanillin composites with antimicrobial properties. *Food Hydrocolloids*, *48*, 62–71. https://doi.org/10.1016/J.FOODHYD.2015.02.008

Swamy, M. K., Sinniah, U. R., & Ghasemzadeh, A. (2018). Anticancer potential of rosmarinic acid and its improved production through biotechnological interventions and functional genomics. *Applied Microbiology and Biotechnology 2018 102:18*, *102*(18), 7775–7793. https://doi.org/10.1007/S00253-018-9223-Y

Wajda, A., Bułat, K., & Sitarz, M. (2016). Structure and microstructure of the glasses from NaCaPO4–SiO2 and NaCaPO4–SiO2–AlPO4 systems. *Journal of Molecular Structure*, *1126*, 47–62. https://doi.org/10.1016/J.MOLSTRUC.2015.12.003

Wajda, A., Goldmann, W. H., Detsch, R., Grünewald, A., Boccaccini, A. R., & Sitarz, M. (2018). Structural characterization and evaluation of antibacterial and angiogenic potential of gallium-containing melt-derived and gel-derived glasses from CaO-SiO2 system. *Ceramics International*, *44*(18), 22698–22709. https://doi.org/10.1016/J.CERAMINT.2018.09.051

Xavier, C. P. R., Lima, C. F., Fernandes-Ferreira, M., & Pereira-Wilson, C. (2009). Salvia Fruticosa, Salvia Officinalis, and Rosmarinic Acid Induce Apoptosis and Inhibit Proliferation of Human Colorectal Cell Lines: The Role in MAPK/ERK Pathway. *Http://Dx.Doi.Org/10.1080/01635580802710733*, *61*(4), 564–571. https://doi.org/10.1080/01635580802710733

Xu, C., Zhan, W., Tang, X., Mo, F., Fu, L., & Lin, B. (2018). Self-healing chitosan/vanillin hydrogels based on Schiff-base bond/hydrogen bond hybrid linkages. *Polymer Testing*, *66*, 155–163. https://doi.org/10.1016/J.POLYMERTESTING.2018.01.016

Yuliarti, O., Hoon, A. L. S., & Chong, S. Y. (2017). Influence of pH, pectin and Ca concentration on gelation properties of low-methoxyl pectin extracted from Cyclea barbata Miers. *Food Structure*, *11*, 16–23. https://doi.org/10.1016/J.FOOSTR.2016.10.005

Zagrajczuk, B., Dziadek, M., Olejniczak, Z., Cholewa-Kowalska, K., & Laczka, M. (2017). Structural and chemical investigation of the gel-derived bioactive materials from the SiO2–CaO and SiO2-CaO-P2O5 systems. *Ceramics International*, *43*(15), 12742–12754. https://doi.org/10.1016/J.CERAMINT.2017.06.160

Zhang, M., Yang, M., Woo, M. W., Li, Y., Han, W., & Dang, X. (2021). High-mechanical strength carboxymethyl chitosan-based hydrogel film for antibacterial wound dressing. *Carbohydrate Polymers*, *256*, 117590. https://doi.org/10.1016/J.CARBPOL.2020.117590

Zhang, Y., Shi, X., Yu, Y., Zhao, S., Song, H., Chen, A., & Shang, Z. (2014). Preparation and Characterization of Vanillin Cross-Linked Chitosan Microspheres of Pterostilbene. *Http://Dx.Doi.Org/10.1080/1023666X.2014.864488*, *19*(1), 83–93. https://doi.org/10.1080/1023666X.2014.864488

Zhou, R., Si, S., & Zhang, Q. (2012). Water-dispersible hydroxyapatite nanoparticles synthesized in aqueous solution containing grape seed extract. *Applied Surface Science*, *258*(8), 3578–3583. https://doi.org/10.1016/J.APSUSC.2011.11.119

Declaration of interests

☐ The authors declare that they have no known competing financial interests or personal relationships that could have appeared to influence the work reported in this paper.

☐The authors declare the following financial interests/personal relationships which may be considered as potential competing interests: